Shear Band Behavior Simulations In Granular Materials Using Weak Discontinuities In A Hypoplastic Constitutive Model

By

Daniel Felipe Castilla Díaz

Adviser

Arcesio Lizcano Ph.D.

Universidad de los Andes

Faculty of Engineering

Civil and Environmental Engineering Department

2009

Index

List of Figures

List of Tables

Chapter 1

Introduction

The shear band in a phenomenon that occurs quite often in soils. Could be on foundations such as footings, slopes or even in laboratory tests, the shear band has an important role in the response of the soils when loading solicitations. Due to its importance, it is necessary to find tools which may help describing the behavior of the shear band.

In macroscopic constitutive models, and specifically in hypoplasticity, the domain is consider to be continuum, with a mean strain field and no singularities. Keeping this in mind, is necessary to develop an extension to the original model, in order to describe the behavior of the shear band.

There are many ways to describe the response of the material after the localization has occurred. COSSERAT's continuum applied to the hypoplastic model to work with a micro polar constitutive model, or with higher-order strain gradient extensions are two of the ways to describe the shear band. But this methodologies are quite complex as well as mathematically and difficult to program at any computer's implementation. That is why a simpler approach is appropriate to make an easy and reliable simulation of the soil's behavior. By using a concept from fracture mechanics called "weak/strong discontinuities", a simpler formulation of the problem can be made, now that the equations are easier to be implemented and to be understood.

In that order of ideas, this works illustrates an explanation of the hypoplastic model and how to implement at a computer's environment. Then comes the concept called bifurcation, that is the point that separates the behavior of the soil in before and after localization as well as how to be implemented; finally how to apply the weak discontinuities theory to soils, how to implement it, along with simulations done within the implementation.

Chapter 2

Hypoplastic Constitutive Model

This chapter presents a brief explanation of the hypoplastic constitutive model, along with its basic properties. Then the variables and additional functions of the VON WOLFFERSDORFF's hypoplastic model, are explained as follows in order to be able to develop a users subroutine (UMAT) for the software ABAQUS. This implementation will be described in the next chapter.

2.1 Hypoplasticity

In general, the constitutive equation in rate form is represented as:

$$\dot{\sigma} = \mathbb{C} : \dot{\varepsilon} \tag{2.1.1}$$

For Hypoplasticity, the basic constitutive equation is:

$$\overset{\circ}{\mathbf{T}} = \mathbb{C}^{hyp} : \mathbf{D} \tag{2.1.2}$$

The hypoplastic general equation is given in rate form:

$$\overset{\circ}{\mathbf{T}} = \mathbf{h}(\mathbf{T}, \mathbf{D}) \tag{2.1.3}$$

Where $\overset{\circ}{\mathbf{T}}$ is the ZAREMBA-JAUMANN objective stress rate tensor, $\mathbf{T}$ is the CAUCHY stress tensor, $\mathbf{D}$ is the stretching or strain rate tensor, and $\mathbf{h}$ is an isotropic tensorial function of $\mathbf{T}$ and $\mathbf{D}$.

According to experimental observations, the hypoplastic model has to satisfy certain properties of the granular materials.

- The behavior is rate independent: The velocity of the load application does not affect the response of the material. This property can be represented mathematically by stating that **h** is positively homogenous in **D**'s first degree.

$$\mathbf{h}(\mathbf{T},\lambda\mathbf{D}) = \lambda\mathbf{h}(\mathbf{T},\mathbf{D}) \quad \forall \quad \lambda > 0 \tag{2.1.4}$$

- According to the experimental behavior observed by GOLDSCHEIDER (1982), a proportional strain (stress) path starting from a nearly stress free state, leads to a proportional stress (strain) path. Mathematically, this means that **h** is homogenous in m degree of **T**

$$\mathbf{h}(\lambda\mathbf{T},\mathbf{D}) = \lambda^m\mathbf{h}(\mathbf{T},\mathbf{D}) \quad \forall \quad \lambda > 0 \quad \text{and} \quad 0 < m \leq 1 \tag{2.1.5}$$

- The constitutive model must have into account the plastic deformations. This means that the loading and unloading paths must be different.

$$\mathbf{h}(\mathbf{T},-\mathbf{D}) \neq -\mathbf{h}(\mathbf{T},\mathbf{D}) \tag{2.1.6}$$

The constitutive equation proposed by KOLYMBAS and WU (1990) and WU (1992) satisfies these three properties:

$$\overset{\circ}{\mathbf{T}} = \mathscr{L}(\mathbf{T},\mathbf{D}) + \mathbf{N}(\mathbf{T}) \parallel \mathbf{D} \parallel \tag{2.1.7}$$

where $\mathscr{L}$ is the fourth order hypoelastic tensor, linear in **D**. **N** is the second order stiffness tensor, nonlinear in **D**. $\parallel \mathbf{D} \parallel$ is the Euclidean norm of **D**

Due to the second term of 2.1.7 $\mathbf{N}(\mathbf{T}) \parallel \mathbf{D} \parallel$, the constitutive equation is incrementally nonlinear. Since $\mathscr{L}$ is linear in **D**, according to WU and BAUER (1999) the equation can be rewritten as:

$$\overset{\circ}{\mathbf{T}} = [\mathscr{L}(\mathbf{T}) + \mathbf{N}(\mathbf{T}) \otimes \bar{\mathbf{D}}] : \mathbf{D} \tag{2.1.8}$$

$$\bar{\mathbf{D}} = \frac{\mathbf{D}}{\parallel \mathbf{D} \parallel} \tag{2.1.9}$$

The fourth order tensor $\mathscr{L}(\mathbf{T}) + \mathbf{N}(\mathbf{T}) \otimes \bar{\mathbf{D}}$ is the tangential stiffness of the material and it depends on the stress state **T** and the normalized stretching $\bar{\mathbf{D}}$. For $\bar{\mathbf{D}} = -\mathbf{D}$, $\overset{\circ}{\mathbf{T}}(\mathbf{T},-\mathbf{D}) = [\mathscr{L} - \mathbf{N} \otimes \bar{\mathbf{D}}] : -\mathbf{D}$, so $\overset{\circ}{\mathbf{T}}(\mathbf{T},-\mathbf{D}) \neq \overset{\circ}{\mathbf{T}}(\mathbf{T},\mathbf{D})$

The fourth order tensor $\mathscr{L}$ must be restricted to limit states, where there are strains ($\mathbf{D} \neq 0$) without stress increments ($\overset{\circ}{\mathbf{T}} = 0$).

$$\bar{\mathbf{D}} = \mathscr{L}(\mathbf{T})^{-1} : \mathbf{N}(\mathbf{T}) \tag{2.1.10}$$

Therefore, $\mathscr{L}^{-1}$ must exist. If $\| \mathbf{D} \|^2 = \dfrac{\mathbf{D} : \mathbf{D}}{\| \mathbf{D} \|^2} = 1$,

$$f(\mathbf{T}) = \| \mathscr{L}^{-1}(\mathbf{T}) : \mathbf{N}(\mathbf{T}) \|^2 - 1 = 0 \tag{2.1.11}$$

$f(\mathbf{T}) = 0$ is the limit stress state, which may be represented as a surface in the stress space $(\mathbf{T}_{11}, \mathbf{T}_{22}, \mathbf{T}_{33})$; and for any stress state lower than the limit $f(\mathbf{T}) < 0$. To decrease stress states 2.1.10 can be associated with the elastoplastic models flow rule.It is important to remark that in hypoplasticity, the limit state is included in the model formulation.

2.1.1 Limit State Surface

BAUER (1996) proposed the following equations for the $\mathscr{L}$ and $\mathbf{N}$ tensors:

$$\mathscr{L}(\hat{\mathbf{T}}) = \hat{a}^2 \mathbb{I} + \hat{\mathbf{T}} \otimes \hat{\mathbf{T}} \quad , \quad \mathbf{N} = \hat{a}(\hat{\mathbf{T}} + \hat{\mathbf{T}}^*) \tag{2.1.12}$$

These equations are functions of the "normalized" stress $\hat{\mathbf{T}} = \dfrac{\mathbf{T}}{\mathrm{Tr}[\mathbf{T}]}$ and the "normalized" deviator stress $\hat{\mathbf{T}}^* = \hat{\mathbf{T}} - \frac{1}{3}$. $\mathbb{I}$ is the fourth order unit tensor and $\hat{a}$ is a positive constant. Once again, $\mathscr{L}$ is invertible:

$$\mathscr{L}^{-1} = \frac{1}{\hat{a}^2}\mathbb{I} - \frac{\hat{\mathbf{T}} \otimes \hat{\mathbf{T}}}{\hat{a}^2(\hat{a}^2 + \| \hat{\mathbf{T}} \|^2)} \tag{2.1.13}$$

By using the previous representation for the $\mathscr{L}$ and $\mathbf{N}$ tensors, the equation for the limit state can be rewritten as:

$$f(\hat{\mathbf{T}}) = \| \mathscr{L}^{-1} : \mathbf{N} \|^2 - 1 = \| \frac{1}{\hat{a}}(\hat{\mathbf{T}} + \hat{\mathbf{T}}^*) - \frac{\| \hat{\mathbf{T}} \|^2 + \| \hat{\mathbf{T}}^* \|^2}{\hat{a}(\hat{a}^2 + \| \hat{\mathbf{T}} \|^2)} \hat{\mathbf{T}} \|^2 - 1 \tag{2.1.14}$$

If $\| \hat{\mathbf{T}} \|^2 = \| \hat{\mathbf{T}}^* \|^2 + \frac{1}{3}$, then the previous equation is simplified to:

$$(\hat{a}^2 - \frac{1}{3}) \| \hat{\mathbf{T}}^* \|^4 - (2\hat{a}^4 + \frac{1}{9}) \| \hat{\mathbf{T}}^* \|^2 + (\hat{a}^6 + \frac{\hat{a}^4}{3} + \frac{\hat{a}^2}{9}) = 0 \tag{2.1.15}$$

This equation has only one positive solution for $\| \hat{\mathbf{T}}^* \|$, which is:

$$\| \hat{\mathbf{T}}^* \| = \hat{a}^2 \tag{2.1.16}$$

If the value of $\hat{a}$ is supposed as a constant, then the limit surface in the stress space is a cone with its tip localized in the origin. In the π plane, which is the perpendicular plane to the isotropic stress line in the stress space, the surface is a circle with radius $\hat{a}$. This corresponds to the DRUCKER-PRAGER limit condition. Figure 2.1 corresponds to this limit surface.

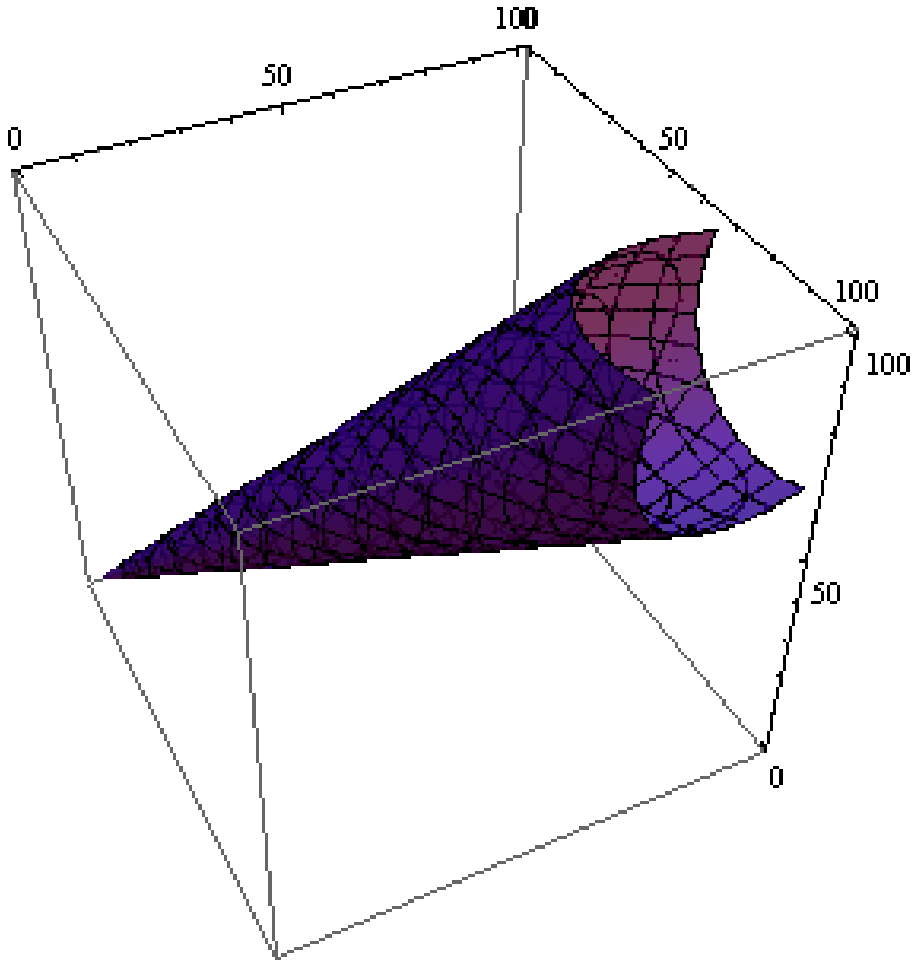

Figure 2.1: DRUCKER-PRAGER limit condition in the stress space

Due to this, the following equation can be determined, using equation 2.1.11:

$$\bar{\mathbf{D}} = -\frac{\hat{\mathbf{T}}^*}{\hat{a}} \tag{2.1.17}$$

This means that for the limit state, $\mathbf{T}$ is proportional to $\hat{\mathbf{T}}^*$. If $\mathrm{Tr}[\mathbf{D}] = -\dfrac{\mathrm{Tr}\left[\hat{\mathbf{T}}^*\right]}{\hat{a}} = 0$, the critical state proposed by CASAGRANDE (1936) and SCHOFIELD and WROTH (1968) characterized by the simultaneous decrease of the stress and the strain rates as well as to deformations with no volumetric change, is described by the constitutive model. BAUER (1995) introduces the relationship between the critic and limit states with the requirement of $\mathrm{Tr}\left[\bar{\mathbf{D}}\right] = \mathrm{Tr}[\mathscr{L} : \mathbf{N}] = 0$.

2.2 VON WOLFFERSDORFF **Hypoplasticity**

This hypoplastic model is an extension of the original model and includes the void ratio e as a variable state. By experimental observation, it can be affirmed that there is not an unique relation between a stress and a void ratio. The range of possible void ratio is delimited by a superior and an inferior limit, and that range decreases when the pressure increases, like it is shown in figure 2.2. The superior limit is the void ratio obtained in an isotropic compression starting from the loosest state with granular contact.

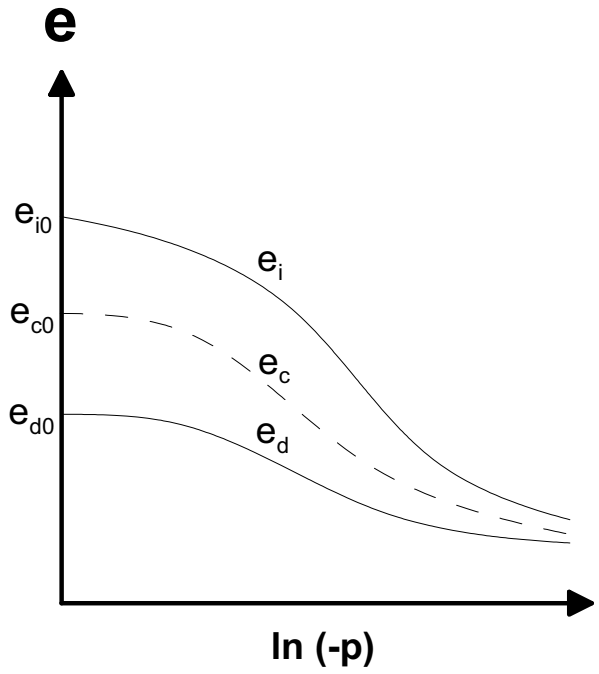

Figure 2.2: Experimental behavior of sand

Three parameters of the material are introduced, the minimum, critical and maximum void ratio (e_i,e_c,e_d). BAUER proposed an equation that adjusts to the experimental behavior of gran-

ular materials, introducing two more material parameters h_s and n, *solid hardness* and *curvature* respectively:

$$\frac{e_i}{e_{i0}} = \frac{e_c}{e_{c0}} = \frac{e_d}{e_{d0}} = \exp\left(-(3p)/h_s\right)^n \tag{2.2.1}$$

The VON WOLFFERSDORFF hypoplastic equation is

$$\overset{\circ}{\mathbf{T}} = \mathscr{L} : \mathbf{D} + f_d \mathbf{N} \parallel \mathbf{D} \parallel \tag{2.2.2}$$

and the void ratio evolution is given by the equation

$$\dot{e} = (1+e)\mathrm{Tr}\left[\mathbf{D}\right] \tag{2.2.3}$$

which means that the change in the void ratio depends only of the volumetric deformation. This implies that the change in the grains volume is 0.

$$\mathscr{L} = \frac{f_s}{\hat{\mathbf{T}} : \hat{\mathbf{T}}} * a^2 \left[\left(\frac{F}{a} \right)^2 \mathbb{I} + \hat{\mathbf{T}} \otimes \hat{\mathbf{T}} \right] \tag{2.2.4}$$

$$\mathbf{N} = \frac{f_s}{\hat{\mathbf{T}} : \hat{\mathbf{T}}} a^2 \left(\frac{F}{a} \right) (\hat{\mathbf{T}} + \hat{\mathbf{T}}^*) \tag{2.2.5}$$

where

$$\mathbb{I} = \frac{1}{2}(\delta_{ik}\delta_{jl} + \delta_{il}\delta_{jk}) \tag{2.2.6}$$

The density factor f_d is a function of the void ratio and the mean stress p:

$$f_d = \left(\frac{e - e_d}{e_c - e_d} \right)^\alpha \tag{2.2.7}$$

The stiffness factor f_s can be decomposed in two parts. The barotropy or the dependant stress factor, and the picnotropy or the dependant void ratio factor. The picnotropy factor causes an increase in the stiffness through the decrease of the void ratio.

$$f_e = \left(\frac{e_i}{e} \right)^\beta \tag{2.2.8}$$

For the isotropic and homogenous condition and starting from a nearly stress free state with

granular contact, $e = e_i$ and $f_e = 1$

$$-3p = 3f_b \left[-a^2 - \frac{1}{3} + \frac{a}{\sqrt{3}} \left(\frac{e_{i0} - e_{d0}}{e_{c0} - e_d 0} \right)^{\alpha} \right] \tag{2.2.9}$$

and

$$-3p = -\frac{1+e_i}{e_i} \frac{h_s}{n} \left(\frac{3p}{h_s} \right)^{1-n} \tag{2.2.10}$$

By replacing 2.2.9 in 2.2.10, the barotropy factor can be obtained:

$$f_b = \frac{e_{i0}}{e_{c0}} \frac{h_s}{n} \frac{1+e_i}{e_i} \left(\frac{-3p}{h_s} \right)^{1-n} \left[3 + a^2 - a\sqrt{3} \left(\frac{e_{i0} - e_{d0}}{e_{c0} - e_{d0}} \right)^{\alpha} \right]^{-1} \tag{2.2.11}$$

2.2.1 Limit Surface - MATSOUKA - NAKAI (1977)

The scalar a in the constitutive equation is related to the limit condition in the critic state. BAUER (1995,1996,1997,2000) proposes that the hypoplastic constitutive equation must not change its general form in order to represent the limit conditions with the adequate interpolation of a. VON WOLFFERSDORFF incorporates the MATSUOKA - NAKAI (1977) limit condition (Figure 2.4). The MATSUOKA - NAKAI limit condition is composed by two parts. First, is the radius of the surface a, which is the same for the DRUCKER - PRAGER limit condition. The second part is the shape factor F, which depends mostly of the deviator stress (Lode's angle and ψ angle) (Figure 2.3). Its function is to change the value of the limit surface, according to the stress path.

$$a = \frac{\sqrt{3}\,(3 - \sin(\phi_c))}{2\sqrt{2}\sin(\phi_c)} \tag{2.2.12}$$

$$F = \sqrt{\frac{1}{8}\tan^2(\psi) + \frac{2 - \tan^2(\psi)}{2 + \sqrt{2}\tan(\psi)\cos(3\theta)}} - \frac{1}{2\sqrt{2}}\tan(\psi) \tag{2.2.13}$$

$$\tan(\psi) = \sqrt{3} \parallel \hat{\mathbf{T}}^* \parallel \tag{2.2.14}$$

$$\cos(3\theta) = -\sqrt{6}\frac{\mathrm{Tr}\left[\hat{\mathbf{T}}^*\right]^3}{\mathrm{Tr}\left[\hat{\mathbf{T}}^{*2}\right]^{\frac{3}{2}}} \tag{2.2.15}$$

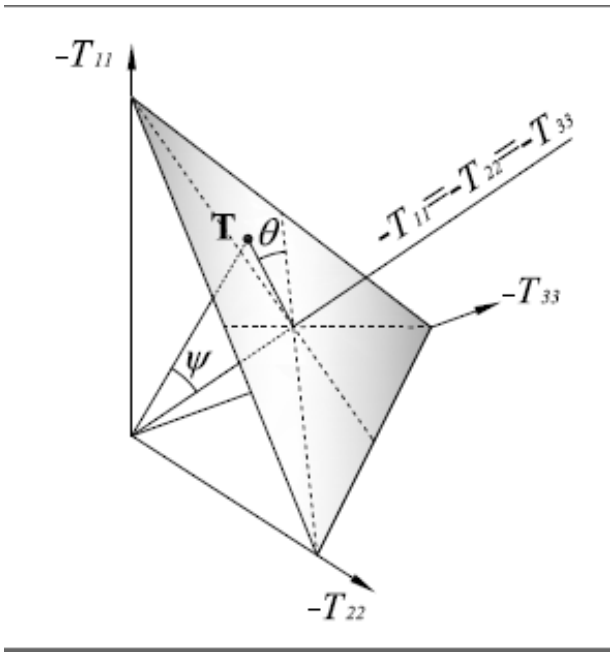

Figure 2.3: Definition of a stress state using θ and ψ. Fuentes (2009)

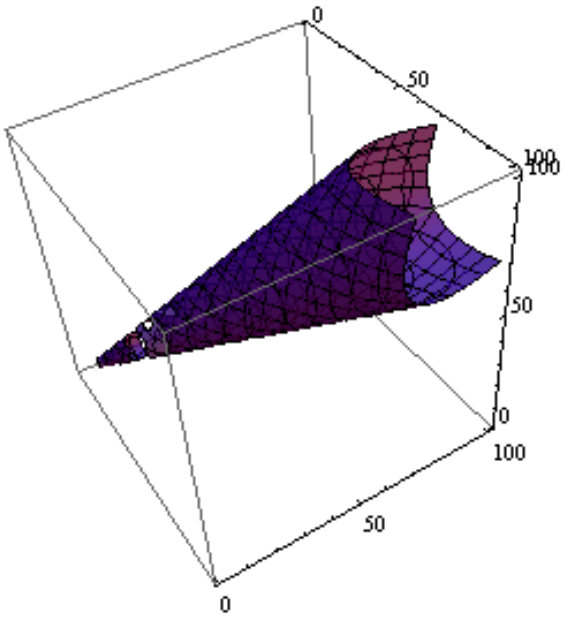

Figure 2.4: MATSUOKA-NAKAI limit surface in the stress space

2.2.2 Hypoplastic Parameters

The hypoplastic constitutive model has eight parameters, and each one has a physical meaning. This means that the parameters are not values proposed to make specific graphics obtained by the model fitting those obtained in laboratory tests, but to represent a physical property or behavior of the material, so the values of the response of the material will be very similar to the real ones. In Arias (2006) [1] there is further information about the parameters and how to obtain them.

2.2.2.1 Critical Friction Angle ϕ_c

The critical friction angle represents the relation between principal stresses in the critical or "stable" state. To obtain ϕ_c it can be assumed that the critical angle and the repose angle of the material are equal. This assumption has been verified by HERLE and GUDEHUS 1999.

2.2.2.2 Reference Void Ratios e_{i0}, e_{c0} and e_{d0}

According to equation 2.2.1, for each stress state there are a maximum, critical and minimal void ratio, and each of these are related to a reference void ratio for a stress state near to zero. According to HERLE and GUDEHUS 1999:

- $e_{d0} = e_{min}$
- $e_{c0} = e_{max}$
- $e_{i0} = 1.15 e_{c0}$

2.2.2.3 Solid Hardness h_s and Curvature Exponent n

The *solid hardness* is related to the volumetric change and is a reference stress of the granular structure of the material, not of one of the grains. It is the only parameter that has units, so there must be consistency with the units. The *curvature exponent* is measurement a of the sensibility of the granular structure to the change in the stress state.

2.2.2.4 α Exponent

The α exponent is a measurement of the stress between the peak state and the stable or critical state. The greater is the ratio between these two states, the exponent increases its value.

2.2.2.5 β Exponent

The β exponent represents how the stiffness of the material is affected by the change in the density. This means that β is related to the barotropy of the material.

Chapter 3

Hypoplasticity - Numerical Implementation (UMAT)

In order to be able to obtain the response of the soil using the Hypoplastic constitutive model, there must be a computer's implementation. In the following chapter there is an explanation on how to implement the model in an UMAT (User-defined mechanical material behavior) in the ABAQUS^{TM}software, using the INCREMENTAL DRIVER as the software used to integrate the UMAT.

3.1 Numerical Implementation Of The Model

In the following section, there is an explanation on the computational implementation of the VON WOLFFERSDORFF hypoplastic equation, which can be used for any software capable of doing the calculations (i.e. MATLAB, MATHEMATICA,MICROSOFT EXCEL). The tensors are supposed as symmetric, so there is a simplification in the representation, transforming the nine components, from the second place tensor to a vector of six components and the eighty one components of the fourth place tensor to 6X6 matrix, as it was explained on the second chapter.

The stresses or strains for any given step are given by either the initial, actual or frontier conditions; or the INCREMENTAL DRIVER in the UMAT implementation. The void ratio is a variable state, and its evolution is calculated using equation 2.2.3.

1. Define the eight parameters (ϕ_c,e_{i0},e_{c0},e_{d0},h_s,n,α and β)

2. Calculate the trace of the stress tensor and the normalized stresses. Also the Euclidean norm of the normalized tensors.

$$\hat{\mathbf{T}} = \frac{\mathbf{T}}{\mathrm{Tr}[\mathbf{T}]}$$
$$\hat{\mathbf{T}}^* = \hat{\mathbf{T}} - \tfrac{1}{3}\mathbf{1}$$

3. Calculate the maximum, critical and minimal void ratio for the actual state using BAUER's Law of compression 2.2.1.

$$\frac{e_i}{e_{i0}} = \frac{e_c}{e_{c0}} = \frac{e_d}{e_{d0}} = \exp\left(-(3p)/h_s\right)^n$$

4. Limit state surface factors. The equation for $cos(3\theta)$, has a discontinuity when $\mathrm{Tr}\left[\hat{\mathbf{T}}^{*^2}\right] = 0$, so there must be a special condition in this case.

$$a = \frac{\sqrt{3}\,(3 - \sin(\phi_c))}{2\sqrt{2}\sin(\phi_c)}$$
$$F = \sqrt{\frac{1}{8}\tan^2(\psi) + \frac{2 - \tan^2(\psi)}{2 + \sqrt{2}\tan(\psi)\cos(3\theta)} - \frac{1}{2\sqrt{2}}\tan(\psi)}$$
$$\tan(\psi) = \sqrt{3} \parallel \hat{\mathbf{T}}^* \parallel$$
$$\cos(3\theta) = -\sqrt{6}\frac{\mathrm{Tr}\left[\hat{\mathbf{T}}^*\right]^3}{\mathrm{Tr}\left[\hat{\mathbf{T}}^{*^2}\right]^{\frac{3}{2}}}$$

If $\mathrm{Tr}\left[\hat{\mathbf{T}}^{*^2}\right] = 0$

$$\cos(3\theta) = 1$$

5. Barotropy, picnotropy and density factors

$$f_b = \frac{e_{i0}}{e_{c0}}\frac{h_s}{n}\frac{1+e_i}{e_i}\left(\frac{-3p}{h_s}\right)^{1-n}\left[3 + a^2 - a\sqrt{3}\left(\frac{e_{i0} - e_{d0}}{e_{c0} - e_{d0}}\right)^{\alpha}\right]^{-1}$$
$$f_e = \left(\frac{e_i}{e}\right)^{\beta}$$
$$f_d = \left(\frac{e - e_d}{e_c - e_d}\right)^{\alpha}$$

6. Linear and non-linear stiffness tensors $\mathscr{L}$ and $\mathbf{N}$

$$\mathscr{L} = \frac{f_s}{\hat{\mathbf{T}} : \hat{\mathbf{T}}} * a^2 \left[\left(\frac{F}{a} \right)^2 \mathbb{I} + \hat{\mathbf{T}} \otimes \hat{\mathbf{T}} \right]$$

$$\mathbf{N} = \frac{f_s}{\hat{\mathbf{T}} : \hat{\mathbf{T}}} a^2 \left(\frac{F}{a} \right) (\hat{\mathbf{T}} + \hat{\mathbf{T}}^*)$$

7. ZAREMBA - JAUMANN stress rate tensor

$$\overset{\circ}{\mathbf{T}} = \mathscr{L} : \mathbf{D} + f_d \mathbf{N} \parallel \mathbf{D} \parallel$$

8. New stress state

$$\mathbf{T}_{n+1} = \mathbf{T}_n + \overset{\circ}{\mathbf{T}} \Delta t$$

3.2 Consistent Tangent Modulus - Numerical Differentiation

The methodology used for the integration of the hypoplastic model is the one presented by FELLIN and OSTERMANN 2002 [4]. In this part, there will be a simpler explanation of the implementation, so people unfamiliar of the concepts or notation are able to implement the constitutive model with the proposed methodology.

First, the implementation of the UMAT is specifically for the software ABAQUS^{TM}, with the INCREMENTAL DRIVER as the software used for the integration. The objective is to find the *Jacobian* $\mathbb{J}$ by the means of a explicit integration. FELLIN and OSTERMANN proposed an approximation of the Jacobian using a numerical differentiation of the consistent tangent modulus.

For an initial stress state $\mathbf{T}(t_a)$ and a strain increment $\Delta\varepsilon$ the UMAT must give the new stress state $\mathbf{T}(t_a + \Delta t)$ and its derivative with respect to the strain increment. In the time $0 \leq t \leq \Delta t$ the following equations must be solved [4]:

$$\frac{d}{dt}\mathbf{T} = \mathbf{h}(\mathbf{T}, \mathbf{D}, \mathbf{Q}) \quad \mathbf{T}(0) = \mathbf{T}(t_a), \frac{d}{dt}\mathbf{Q} = \mathbf{k}(\mathbf{T}, \mathbf{D}, \mathbf{Q}) \quad \mathbf{Q}(0) = \mathbf{Q}_0 \tag{3.2.1}$$

$\mathbf{Q}$ represents the additional state variables, which in this case is only one, the void ratio e. By solving simultaneously the equations mentioned before, with the Jacobian being:

$$\frac{\partial \Delta\sigma}{\partial \Delta\varepsilon} = \frac{1}{\Delta t}\frac{\partial \mathbf{T}}{\partial \mathbf{D}}(\Delta t) \tag{3.2.2}$$

Using numerical differentiation, by solving the equations is much simpler thus two equations are obtained:

$$\frac{d}{dt}\mathbf{B}_{ij} = \frac{1}{\vartheta}\left(\mathbf{h}(\mathbf{T}+\vartheta\mathbf{B}_{ij}\mathbf{D}+\vartheta\mathbf{V}_{ij}\mathbf{Q}+\vartheta\mathbf{G}_{ij})-\mathbf{h}(\mathbf{T},\mathbf{D},\mathbf{Q})\right) \quad \mathbf{B}_{ij}(0)=0, \tag{3.2.3}$$

$$\frac{d}{dt}\mathbf{G}_{ij} = \frac{1}{\vartheta}\left(\mathbf{k}(\mathbf{T}+\vartheta\mathbf{B}_{ij}\mathbf{D}+\vartheta\mathbf{V}_{ij}\mathbf{Q}+\vartheta\mathbf{G}_{ij})-\mathbf{k}(\mathbf{T},\mathbf{D},\mathbf{Q})\right) \quad \mathbf{G}_{ij}(0)=0, \tag{3.2.4}$$

with $1 \leq i,j \leq 3$ and $\mathbf{V}_{ij} = (\delta_{ik}\delta_{jl})_{k,l=1}^{3}$.

Using a TAYLOR expansion, the following equation is obtained

$$\mathbf{B}_{ij} = \frac{\partial \mathbf{T}}{\mathbf{D}_{ij}} + f(\vartheta) \tag{3.2.5}$$

The $\mathbf{B}_{ij}$ tensors are very good numerical approximations of the Jacobian, when the ϑ parameter is sufficiently small. Thus, and specifically for double precision variables

$$\vartheta = \max(1, \| \mathbf{D} \|)\sqrt{10^{-15}} \tag{3.2.6}$$

In order to solve the equations, all the variables are collected in a "super vector" called y

$$\mathbf{y} = (\mathbf{T}_1, \mathbf{T}_2, ..., \mathbf{T}_6, (\mathbf{B}_1)_1, (\mathbf{B}_1)_2 ..., (\mathbf{B}_1)_6, (\mathbf{B}_2)_1, (\mathbf{B}_2)_2, ..., (\mathbf{B}_2)_6, ..., (\mathbf{B}_6)_6, \mathbf{Q}_1, ..., \mathbf{Q}_n, (\mathbf{G}_1)_1, ..., (\mathbf{G}_6)_n) \tag{3.2.7}$$

And the rate of this vector is calculated like

$$y = y + \dot{y} \cdot h \tag{3.2.8}$$

Being h

$$h = \frac{\Delta t}{tsub}, \quad tsub = \text{Size of the sub step} \tag{3.2.9}$$

And

$$\dot{y} = \frac{\dot{\mathbf{T}}(t_a + \Delta t) - \dot{\mathbf{T}}(t_a)}{\vartheta} \tag{3.2.10}$$

$$\dot{y} = \frac{\dot{e}(t_a + \Delta t) - \dot{e}(t_a)}{\Delta t} \tag{3.2.11}$$

The equation 3.2.10 is for the evolution of the stresses, and the equation 3.2.11 is for the evolution of the state variables.

Finally, by obtaining the stresses due to an increment in the strains, it is possible to calculate the Jacobian. Then, the values of the Jacobian must be ordered in the way ABAQUS^{TM}requires it.

$$\mathbb{J} = \frac{y}{\Delta t} \tag{3.2.12}$$

3.3 Results

Using the procedure presented above, an UMAT was developed and two types of element test were simulated: A consolidated-undrained (CU) triaxial test, and a consolidated-drained triaxial test (CD). Three void ratios and four confinement pressures were supposed. The void ratios correspond to a dense, mean and loose state. The material properties used for the simulation are the parameters for Guamo's sand, determined by Arias (2006) [1].

Variable	Value
ϕ_c	30°
e_{i0}	1.15
e_{c0}	1.00
e_{d0}	0.52
h_s	4000000 kPa
n	0.27
α	0.17
β	1

Table 3.1: Guamo's sand hypoplastic parameters

3.3.1 CU Triaxial Test

For the CU triaxial test, two graphics were made: Deviator stress vs. axial strain, and deviator tress vs. mean stress. Each graphic represents the four confinement pressures for the same void ratio.

3.3.1.1 Dense State

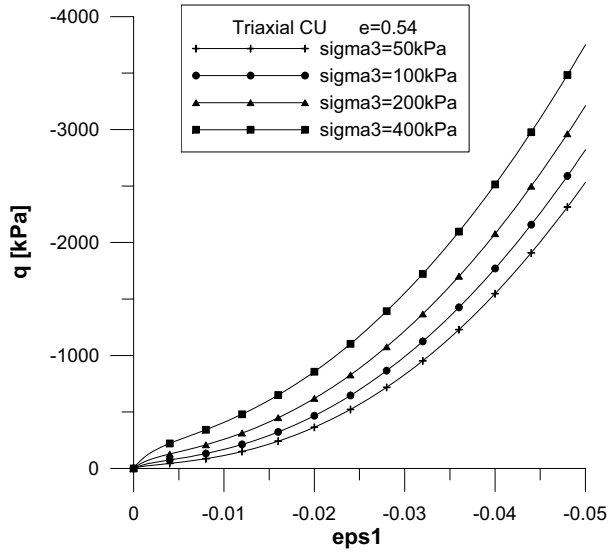

Figure 3.1: CU Triaxial, q vs. ε_1, e=0.54

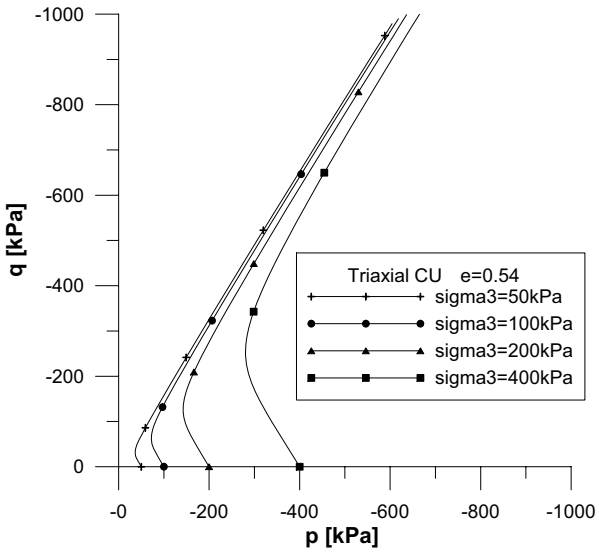

Figure 3.2: CU Triaxial, q vs. p, e=0.54

For the void ratio $e = 0.54$, which means a very dense state, it can be observed in figures 3.1 and 3.2 that the initial stiffness is greater when increasing the confinement pressure. After a peak resistance which is easier to find in the q vs. p graph, the behavior of the material for the different pressures is the same, since it reaches the critical state.

3.3.1.2 Mean State

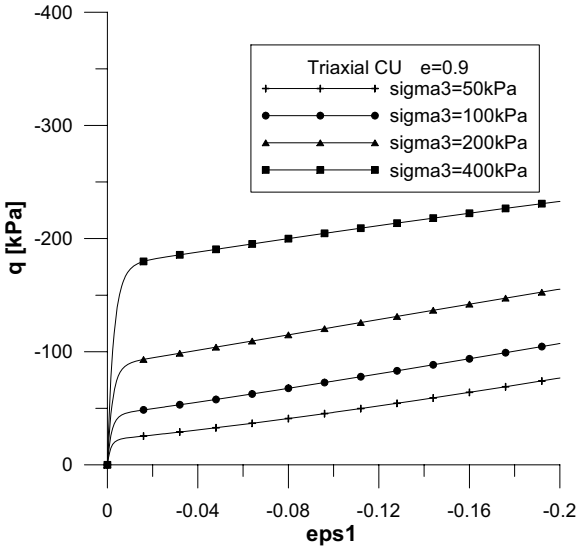

Figure 3.3: CU Triaxial, q vs. ε_1, e=0.9

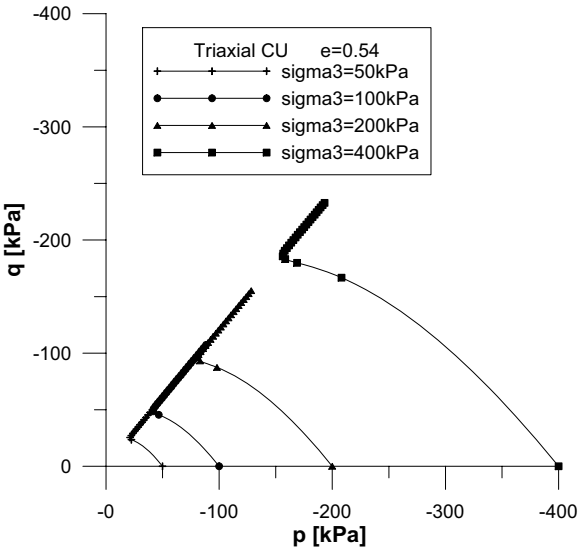

Figure 3.4: CU Triaxial, q vs. p, e=0.9

For the mean state (void ratio e=0.9, figures 3.3 and 3.4), since the void ratio is very close to the reference critical void ratio, the peak resistance is reached at a larger axial strain, and it also reaches the critical state after the peak.

3.3.1.3 Loose State

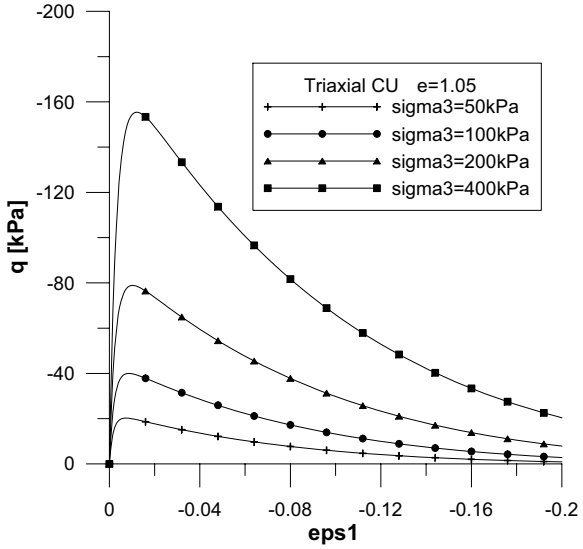

Figure 3.5: CU Triaxial, q vs. ε_1, e=1.05

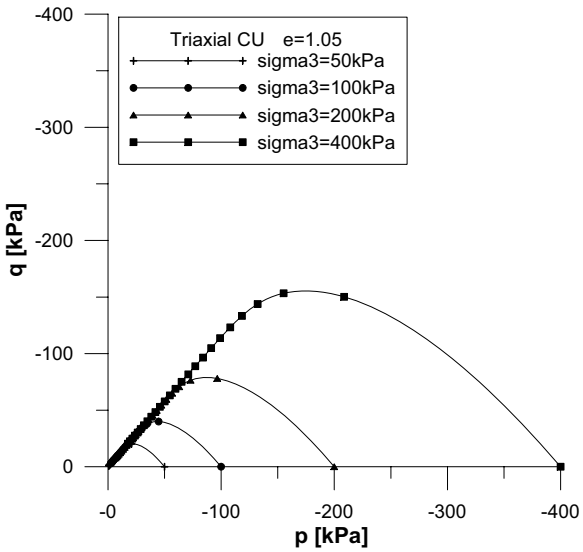

Figure 3.6: CU Triaxial, q vs. p, e=1.05

For the loose state (void ratio e=1.05, figure 3.5 and 3.6), the void ratio is larger than the critical void ratio. The peak resistance increases with the confinement pressure, and after the peak, the material softens very quickly, reaching the critical state. It has a clear difference between the behaviors of the material regarding dense with the mean state, because in loose and mean states, the material experiments hardening, while in the loose state, the phenomenon taking place is softening.

3.3.2 CD Triaxial Test

For the Consolidated-Drained triaxial test, four graphics are presented for each value of initial void ratio: Deviator stress vs. axial strain, deviator stress vs. mean stress, deviator stress vs. void ratio, and volumetric strain vs. axial strain.

3.3.2.1 Dense State

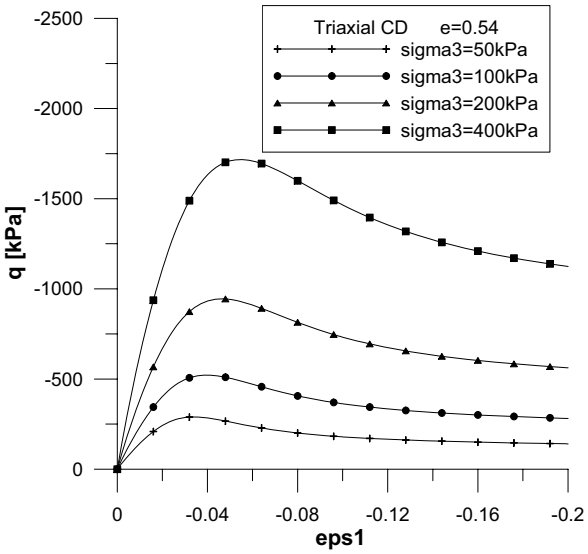

Figure 3.7: CD Triaxial, q vs. ε_1, e=0.54

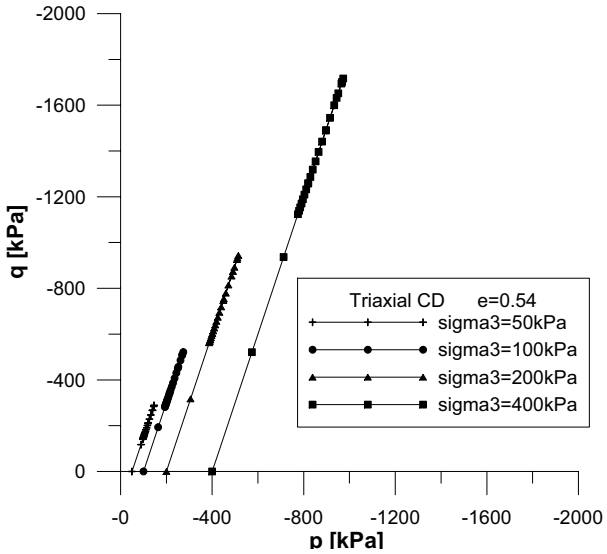

Figure 3.8: CD Triaxial, q vs. p, e=0.54

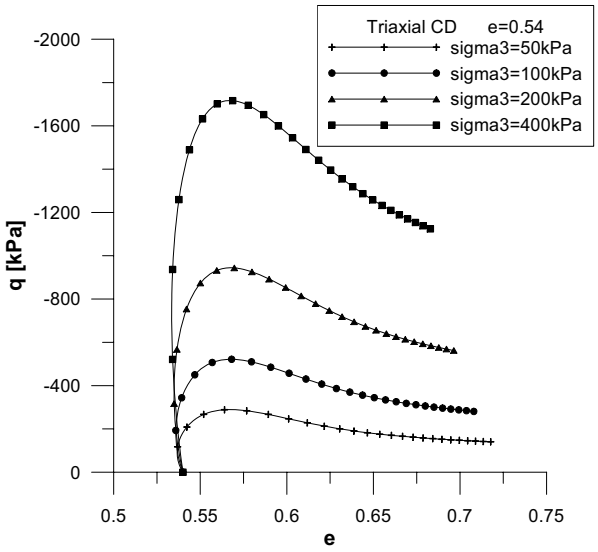

Figure 3.9: CD Triaxial, q vs. e, e=0.54

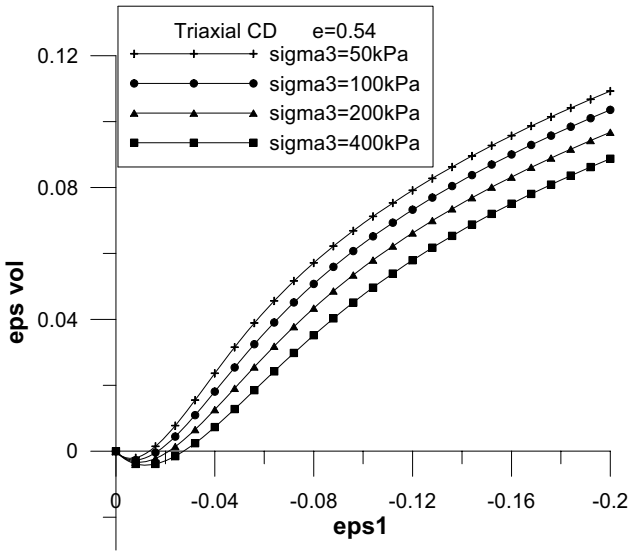

Figure 3.10: CD Triaxial, ε_{vol} vs. ε_1, e=0.54

In the dense state(e=0.54, Figures 3.7, 3.8, 3.9 and 3.10), the resistance has a peak point and then a residual state. It also changes its behavior from contractive to dilatants. The means the volumen first diminishes and then increases until it reaches a stable value.

3.3.2.2 Mean State

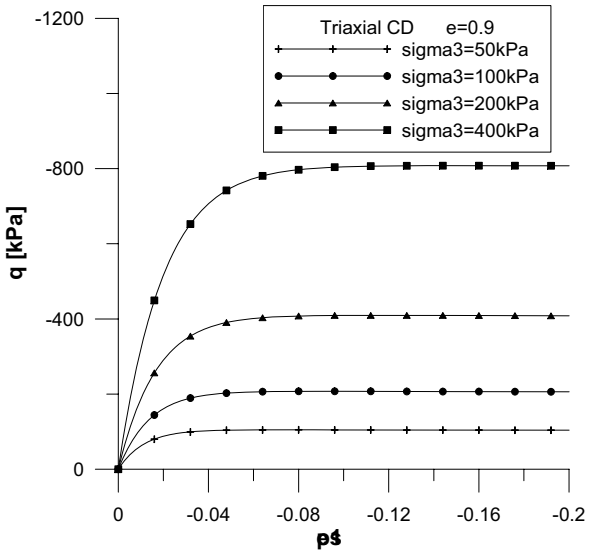

Figure 3.11: CD Triaxial, q vs. ε_1, e=0.9

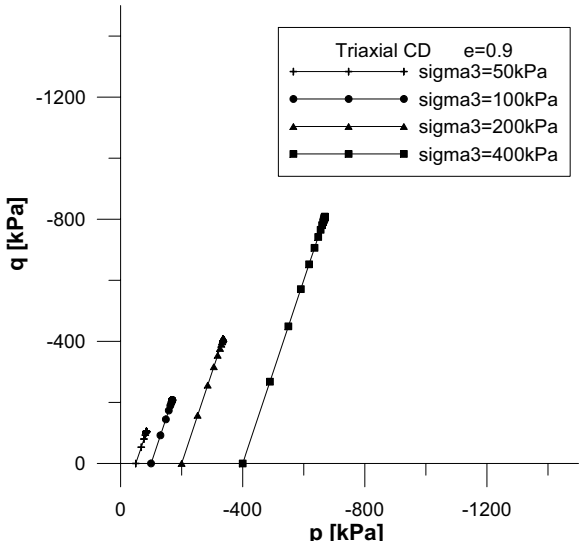

Figure 3.12: CD Triaxial, q vs. p, e=0.9

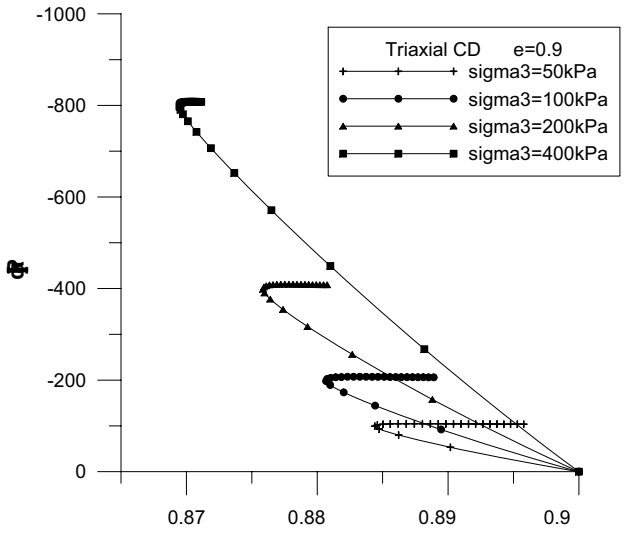

Figure 3.13: CD Triaxial, q vs. e, e=0.9

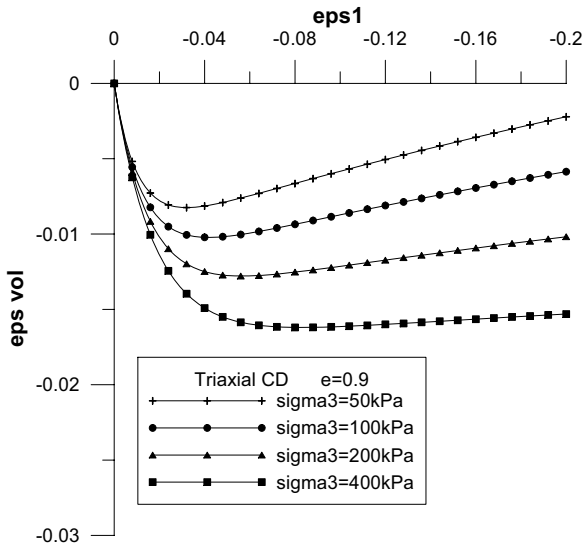

Figure 3.14: CD Triaxial, ε_{vol} vs. ε_1, e=0.9

Due to the proximity of the initial void ratio to the critical void ratio ($e = 0.9$, Figures 3.11, 3.12, 3.13 and 3.14), the material does not evidence a peak resistance. It reaches a stable state which can be associated to the fluency in metals. The volumetric strain rate changes but the volumetric strain

is always negative, meaning that the volume decreases and increases, but the volume is minor than the initial one. With respect to the void ratio, it diminishes to a minimum and it increases to a stable value.

3.3.2.3 Loose State

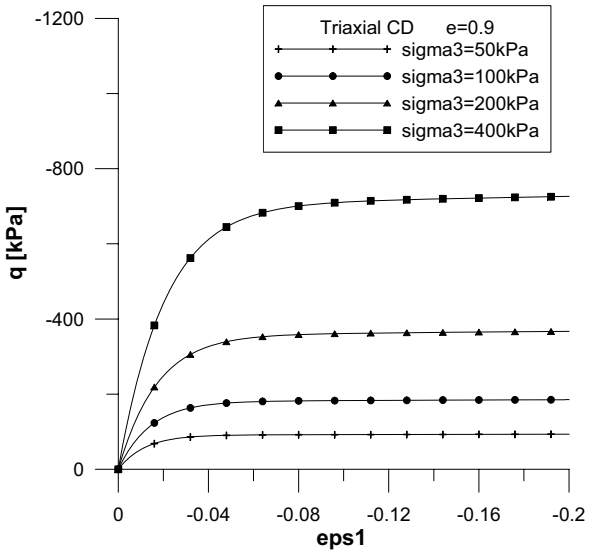

Figure 3.15: CD Triaxial, q vs. ε_1, e=1.05

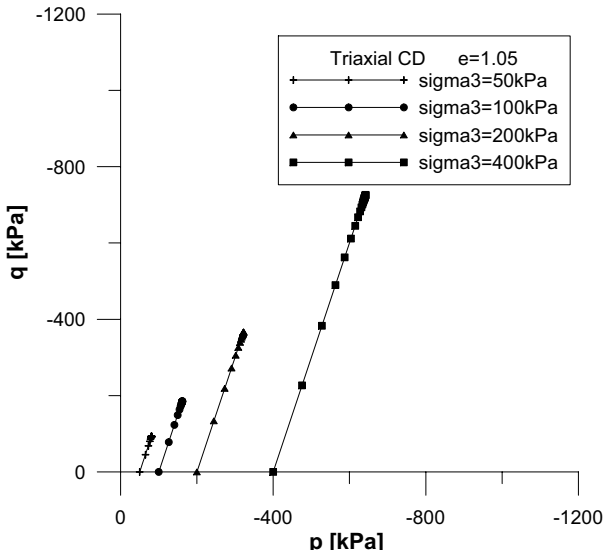

Figure 3.16: CD Triaxial, q vs. p, e=1.05

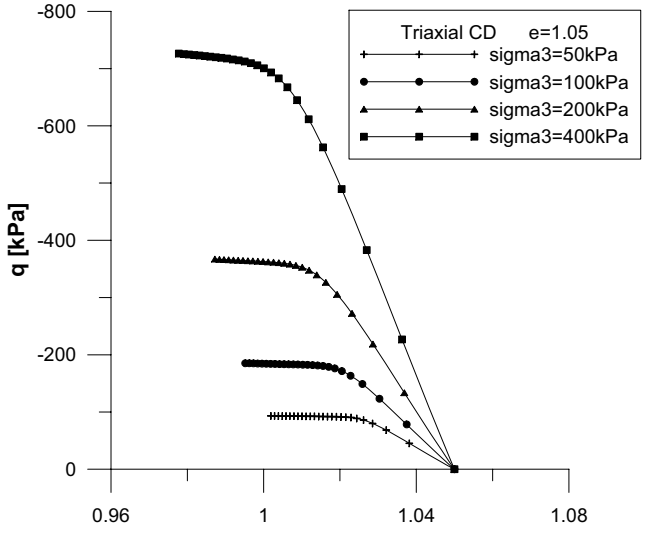

Figure 3.17: CD Triaxial, q vs. e, e=1.05

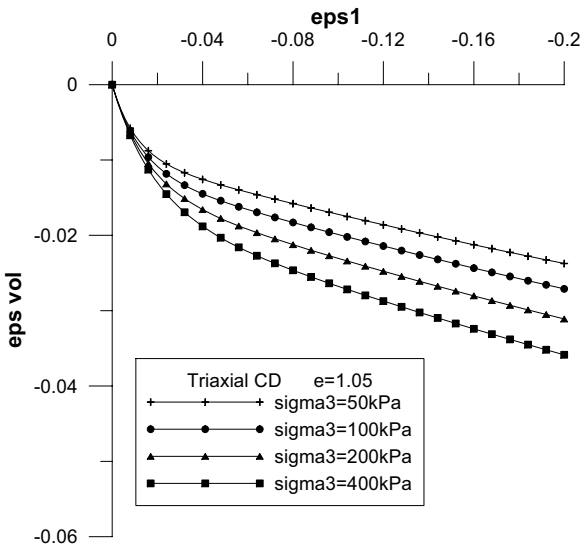

Figure 3.18: CD Triaxial, ε_{vol} vs. ε_1, e=1.05

For the loose state (e=1.05, Figures 3.15, 3.16, 3.17 and 3.18), the behavior is similar to the one on the mean state with respect to the resistance, while in the void ratio and in the volumetric strain the behavior changes. The volume decreases as well as the void ratio, reaching a stable state.

Chapter 4

Bifurcation And Post Bifurcation Behavior - Implementation

4.1 Bifurcation Criterium

In hypoplasticity, being a macroscopic constitutive model, the granular material is assumed as continuum with some intrinsic and variable properties, with no singularities whatsoever. So when a spatial singularity, such as the shear band, needs to be described mathematically, new conditions must be taken into account.

In macroscopic constitutive models like hypoplasticity, strains are calculated as the mean value of the strains, so the stain field is also a mean-valued. But when a singularity appears in the field, this phenomena is called "localized bifurcation". This means that in a specific spatial region, the strain field has a singularity which separates the field in two different parts.

There are several ways to describe the post-localization behavior mathematically, such as COSSERAT Continuum: TEJCHMAN (2008)[12], HUANG (2000)[5]; Strain-gradient extensions: WU (2007)[13]; or Weak-Strong discontinuities approach: OLIVER (2002, 2004) [11] [6] [7]. The method proposed in this work will be discussed later in this chapter.

It is important to remark that the bifurcation criterium is mainly a theorical concept, which comes from a mathematic analysis, and has not been demonstrated physically. First, the localization of the strains is a phenomenon which may or may not occur, therefore it is not a determining concept. Physically, it can be triggered by imperfections or border conditions, while theoretically

it is due to certain stress-strain conditions. Theoretically, the bifurcation only occurs when there is softening due to deformation and before the peak deviator stress.

The methodology used for the localized bifurcation is the one proposed by NIEMUNIS (2003)[10] and BAUER (1999) [2].

4.1.1 Mathematical Formulation

First, is a continuous velocity field with the possibility of a discontinuity in the spatial gradient across a π plane (figure 4.1).

$$\frac{\partial v}{\partial x} \neq 0 \tag{4.1.1}$$

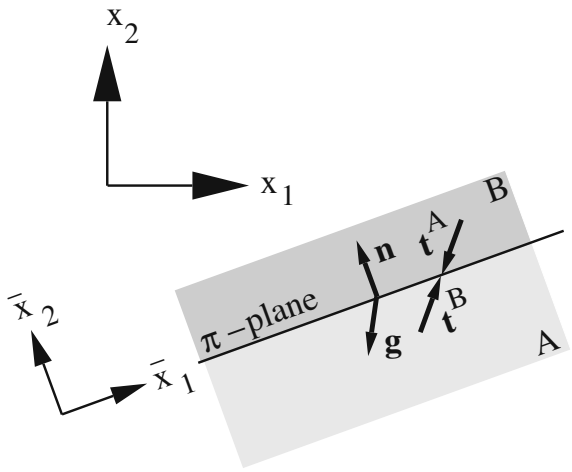

Figure 4.1: π plane in a continuous body. Taken from Niemunis (2003) [10]

The stress field associated with the *pi* plane must be in equilibrium. If there are two different parts separated by the *pi* plane, called **A** and **B**, and each part has a stress rate tensor $\dot{\mathbf{T}}_A$ and $\dot{\mathbf{T}}_B$ and a velocity gradient $\frac{\partial v^A}{\partial x}$ and $\frac{\partial v^B}{\partial x}$ respectively.

For the initial state with $\mathbf{T}_A = \mathbf{T}_B$ and $\dot{\mathbf{T}}_A = \dot{\mathbf{T}}_B$, the jump in the velocity gradient can be written as $\left[\!\left[\frac{\partial v}{\partial x}\right]\!\right] = \left(\frac{\partial v}{\partial x}\right)^B - \left(\frac{\partial v}{\partial x}\right)^A$. Using the MAXWELLś compatibility condition applied to a first order gradient:

$$[\![\varepsilon]\!] = \varepsilon^B - \varepsilon^A = [\![\nabla^s \mathbf{u}]\!] = (\mathbf{g} \otimes \mathbf{n})^s \tag{4.1.2}$$

And for the velocity field

$$\left[\!\left[\frac{\partial v}{\partial x}\right]\!\right] = \mathbf{g} \otimes \mathbf{n} \tag{4.1.3}$$

Being ε the strain field, $\mathbf{u}$ the displacement field, $\mathbf{n}$ the normal vector the π plane, and $\mathbf{g}$ an arbitrary vector. The $\mathbf{g}$ vector cannot be determined by geometric methods. When $\mathbf{g} = 0$, there is no discontinuity because $\mathbf{D}^A = \mathbf{D}^B$.

First, there are two velocity scalar fields $v(x)^A$ and $v(x)^B$, smooth and continuous. The velocity field in the interface is $\pi(x) = 0$ and the continuity condition $v(x)^A = v(x)^B$ is fulfilled in the π plane. A local coordinate system $\bar{X}_1$ and $\bar{X}_2$ is developed, being $\bar{X}_2$ perpendicular to the interface π like is shown in the figure 4.1. The continuity conditions are now:

$$\frac{\partial \bar{v}}{\partial \bar{x_1}}^A = \frac{\partial \bar{v}}{\partial \bar{x_1}}^B \quad \text{and} \quad \frac{\partial \bar{v}}{\partial \bar{x_2}}^A = \frac{\partial \bar{v}}{\partial \bar{x_2}}^B \tag{4.1.4}$$

In the direction $\bar{X}_1$, the divergence of the velocity gradient vanishes, thus the only continuity condition that must be taken into account is the one in the $\bar{X}_2$ direction.

$$\left[\!\left[\frac{\partial \bar{v}}{\partial \bar{x}}\right]\!\right] = \bar{g} \otimes \bar{\mathbf{n}} \tag{4.1.5}$$

Where g is the scalar value of $\mathbf{g}$, and it changes with the direction of π.

$$\bar{g} = \bar{g}(\bar{X}_1, \bar{X}_3) \tag{4.1.6}$$

If this equation is applied to all te components of the velocity $\bar{v}_1$,$\bar{v}_2$ and $\bar{v}_3$ and each one is analyzed as an independent scalar field

$$\left[\!\left[\frac{\partial \bar{v}_1}{\bar{x}}\right]\!\right] = \bar{g}_1 \bar{\mathbf{n}}\,, \quad \left[\!\left[\frac{\partial \bar{v}_2}{\bar{x}}\right]\!\right] = \bar{g}_2 \bar{\mathbf{n}}\,, \quad \left[\!\left[\frac{\partial \bar{v}_3}{\bar{x}}\right]\!\right] = \bar{g}_3 \bar{\mathbf{n}} \tag{4.1.7}$$

And these expressions can be simplified as if each one is a component of the **g** vector:

$$\left[\!\left[\begin{array}{c} \dfrac{\partial \bar{v}_1}{\bar{x}} \\ \dfrac{\partial \bar{v}_2}{\bar{x}} \\ \dfrac{\partial \bar{v}_3}{\bar{x}} \end{array} \right]\!\right] = \begin{bmatrix} 0 \\ 1 \\ 0 \end{bmatrix} \begin{bmatrix} \bar{g}_1 & \bar{g}_2 & \bar{g}_3 \end{bmatrix} = \begin{bmatrix} 0 & \bar{g}_1 & 0 \\ 0 & \bar{g}_2 & 0 \\ 0 & \bar{g}_3 & 0 \end{bmatrix} \tag{4.1.8}$$

The velocity gradient can be separated in two parts: the symmetric and the anti symmetric components parts ($[\![\mathbf{D}]\!]$ and $[\![\mathbf{W}]\!]$).

$$[\![\mathbf{D}]\!] = \frac{1}{2}(\bar{g}\bar{n} + \bar{n}\bar{g}) = \frac{1}{2} \begin{bmatrix} 0 & \bar{g}_1 & 0 \\ \bar{g}_1 & 2\bar{g}_2 & \bar{g}_3 \\ 0 & \bar{g}_3 & 0 \end{bmatrix} \tag{4.1.9}$$

$$[\![\mathbf{W}]\!] = \frac{1}{2}(\bar{g}\bar{n} - \bar{n}\bar{g}) = \frac{1}{2} \begin{bmatrix} 0 & \bar{g}_1 & 0 \\ -\bar{g}_1 & 0 & -\bar{g}_3 \\ 0 & \bar{g}_3 & 0 \end{bmatrix} \tag{4.1.10}$$

The eigenvalues of $[\![\mathbf{D}]\!]$ are $0, \frac{1}{2}(\bar{g}_2 + \sqrt{\bar{g}_1^2 + \bar{g}_2^2 + \bar{g}_3^2})$ and $\frac{1}{2}(\bar{g}_2 - \sqrt{\bar{g}_1^2 + \bar{g}_2^2 + \bar{g}_3^2})$. This means that the jump in the strain rate has a diagonal form.

$$[\![\mathbf{D}]\!] = \text{diag}\left[0, \frac{1}{2}(\bar{n}\bar{g} + [\![\bar{g}]\!]), \frac{1}{2}(\bar{n}\bar{g} - [\![\bar{g}]\!])\right] \tag{4.1.11}$$

The dilatancy angle is now calculated as

$$\frac{\text{Tr}\,[[\![\mathbf{D}]\!]]}{\| [\![\mathbf{D}]\!] \|} = \frac{2 * \bar{n} * \bar{g}}{\sqrt{\bar{n}\bar{g} + \bar{g}\bar{g}}} \tag{4.1.12}$$

The equilibrium condition in the π plane is:

$$[\![\mathbf{t}]\!] = [\![\mathbf{T}]\!]\bar{\mathbf{n}} = 0 \tag{4.1.13}$$

For the initial state, the stress rate field is described by the equation:

$$[\![\dot{\mathbf{t}}]\!] = [\![\dot{\mathbf{T}}]\!]\mathbf{n} + [\![\mathbf{T}]\!]\dot{\mathbf{n}} = 0 \tag{4.1.14}$$

Since $\mathbf{n}$ is constant and its derivative is equal to zero, the equation can be simplified to:

$$[\![\dot{\mathbf{t}}]\!] = [\![\dot{\mathbf{T}}]\!]\mathbf{n} = 0 \tag{4.1.15}$$

If a homogenous stress state is supposed, meaning that the analysis time is when the singularity is starting $[\![\dot{\mathbf{T}}]\!] = 0$. In the local coordinate system:

$$[\![\dot{\mathbf{T}}_{12}]\!] = [\![\dot{\mathbf{T}}_{22}]\!] = [\![\dot{\mathbf{T}}_{23}]\!] = 0 \tag{4.1.16}$$

$[\![\dot{\mathbf{T}}_{11}]\!]$, $[\![\dot{\mathbf{T}}_{13}]\!]$ and $[\![\dot{\mathbf{T}}_{33}]\!]$ can be discontinuous in the π plane.

Since the hypoplastic model is incrementally non-linear, $[\![\dot{\mathbf{T}}]\!]$ cannot be calculated by replacing $[\![\mathbf{D}]\!]$ and $[\![\mathbf{W}]\!]$. Due to the equilibrium condition, the stress rate vectors $\dot{\mathbf{t}}$ in both sides of the plane π must be equal.

$$\dot{\mathbf{T}}^A\bar{n} + \dot{\mathbf{T}}^B(-\bar{n}) = 0 \tag{4.1.17}$$

Therefore

$$[\![\dot{\mathbf{T}}]\!] = 0 \tag{4.1.18}$$

Using the formulation for the ZAREMBA - JAUMANN objective stress rate tensor, the jump in the CAUCHY's stress rate tensor can be calculated like

$$[\![\dot{\mathbf{T}}_{ij}]\!] = [\![\overset{\circ}{\mathbf{T}}_{ij}]\!] - \mathbf{T}_{ik}[\![\mathbf{W}_{kj}]\!] + [\![\mathbf{W}_{ik}]\!]\mathbf{T}_{kj} \tag{4.1.19}$$

and using the formulation from before in matrix notation

$$[\![\mathbf{W}_{ij}]\!] = \frac{1}{2}(g_i n_j - n_i g_j) \; , \; [\![\mathbf{D}_{ij}]\!] = \frac{1}{2}(g_i n_j + n_i g_j) \tag{4.1.20}$$

Accordingly

$$[\![\dot{t}_j]\!] = n_i [\![\dot{\mathbf{T}}_{ij}]\!] + A_{jk} g_k \tag{4.1.21}$$

The **A** tensor is a simplification for the notation, and has the magnitude of stress.

$$2A_{jk} = n_i \mathbf{T}_{ij} n_k - \mathbf{T}_{kj} - n_j n_i \mathbf{T}_{ik} + n_i \mathbf{T}_{ir} n_r \delta_{jk} \; , \; \delta_{jk} \rightarrow \text{Kronecker's Delta} \tag{4.1.22}$$

Using the hypoplastic equation, the equilibrium condition can now be written as

$$(n_i \mathscr{L}_{ijkl} n_l + A_{jk}) g_k + N_{ij} n_i ([\![\mathbf{D}^A]\!] - [\![\mathbf{D}^B]\!]) = 0 \tag{4.1.23}$$

To simplify the notation of the equation, the following simplifications are introduced:

$$\bar{L}_{jk} = n_i \mathscr{L}_{ijkl} n_l + A_{jk} \; , \; \bar{N}_i = N_{ij} n_i \tag{4.1.24}$$

It is important to remark that $\bar{L}_{jk}$ is always positive, because it has the magnitude of stiffness, so it is always larger than A_{jk}.

The bifurcation criterium is fulfilled when the equation

$$\bar{\mathbf{L}}\mathbf{g} + \bar{\mathbf{N}}([\![\mathbf{D}^A]\!] - [\![\mathbf{D}^B]\!]) = 0 \tag{4.1.25}$$

has a solution with $\mathbf{g} \neq 0$. An additional restriction must be imposed to $[\![\mathbf{D}]\!]$ when $[\![\mathbf{D}^A]\!]$ and $[\![\mathbf{D}^B]\!]$ are given. According to WU and SIKORA (1991) [14] the following triangle inequality must be satisfied:

$$\| \, [\![\mathbf{D}^A]\!] - [\![\mathbf{D}^B]\!] \, \| < \| \, [\![\mathbf{D}]\!] \, \| < \| \, [\![\mathbf{D}^A]\!] + [\![\mathbf{D}^B]\!] \, \| \tag{4.1.26}$$

The concept of *Degree of bifurcation* is now introduced and is calculated with the following equation

$$d_b = \frac{\| [\![\mathbf{D}]\!] \|}{\| \mathbf{D}^A \| - \| \mathbf{D}^B \|} \tag{4.1.27}$$

The localization is posible if $d_b = 1$ assuming $[\![\mathbf{D}^A]\!] - [\![\mathbf{D}^B]\!] = 1$ and when the inequality is first satisfied ($\mathbf{D}^A$, $\mathbf{D}^B$ and $\mathbf{D}^A - \mathbf{D}^B$ are proportional).

$$\| \mathbf{D}^A \| - \| \mathbf{D}^B \| = \| [\![\mathbf{D}]\!] \| = \pm \frac{1}{\sqrt{2}} \sqrt{\mathbf{g}\cdot\mathbf{g} + (\mathbf{g}\cdot\mathbf{n})^2} \tag{4.1.28}$$

The bifurcation criterium can be simplified as

$$\bar{\mathbf{L}}\cdot\mathbf{g} = \pm \frac{1}{\sqrt{2}} \sqrt{\mathbf{g}\cdot\mathbf{g} + (\mathbf{g}\cdot\mathbf{n})^2} \tag{4.1.29}$$

where $\mathbf{g}$ is proportional to $\pm\bar{\mathbf{L}}^{-1}\bar{\mathbf{N}}$, and so replacing in the equation, the criterion can be numerically verified using the expression

$$2 = \| \bar{\mathbf{L}}^{-1}\bar{\mathbf{N}} \|^2 + (\mathbf{n}\bar{\mathbf{L}}^{-1}\bar{\mathbf{N}})^2 \tag{4.1.30}$$

4.2 Bifurcation Criteria - Implementation

Since the 4.1.30 equation has no analytic solution, the implementation of the bifurcation criterium must be a subroutine that calculates the right hand side of the equation for all posible inclinations of the shear band and verifies the criterium. The following part is a brief explanation on how to write this part of the implementation.

1. First, all posible directions for the **n** vector must be taken into account. Assuming **n** as a vector characterized by a ϕ and ψ angle, the stress tensor must be rotated so the 1 axis matches the **n** vector (figure 4.2.

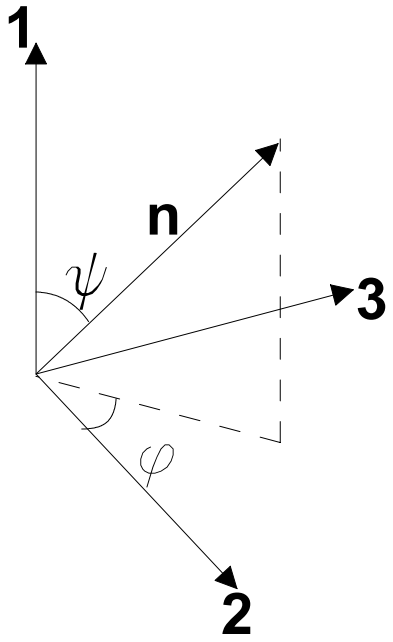

Figure 4.2: Direction of the **n** vector

For the calculations, it is not necessary to use all the possible values for ψ and ϕ since the problem is axisymmetric. Two DO cycles must be created, by first changing the ϕ angle, and then by changing the shear band inclination angle ψ.

2. Once the stress tensor is rotated, the values of the $\mathscr{L}$ and **N** tensors must be calculated using the hypoplastic equation

3. The **A** tensor and therefore the $\bar{\mathbf{L}}$ tensor can be calculated. Also the $\bar{\mathbf{N}}$ vector.

4. The next step is to obtain the inverse of the $\bar{\mathbf{L}}$ tensor so the **g** vector can be calculated

5. The right hand side of the equation 4.1.30 may now be obtained, and so the bifurcation criteria can be verified. For each step of the calculus it is important to save the lowest value of the 4.1.30 equation, since this is the verification of the criterium. When the simulation is completed, the value may be verified to find if bifurcation has occurred.

4.3 Weak Discontinuities - Post Bifurcation Behavior

The shear band in granular materials is a zone within the body that behaves in a different form as the rest of the material. New strains occur in this zone, and macroscopic models, such as hypoplasticity,

cannot describe this behavior, because of its formulation. The body is supposed as a continuous material, isotropic and homogeneous. But since the shear band is a singularity in the material, there must be extensions to the original model, so this particular behavior can be simulated.

There are many ways to develop these extensions, but most of them count with high complexity levels of mathematical procedures and computational complications. COSSERAT's continuum [9] for micro polar hypoplastic models or higher order strain gradient extensions are two ways to describe the post bifurcation behavior, but as it was stated above, its numerical implementation can be incredibly complex and at greater computational costs.

A simpler way to perform this analysis could be one taken from fracture mechanics, called the Weak/Strong discontinuities. Even though its formulation is made for large strains, and the hypoplastic model and the INCREMENTAL DRIVERhave been developed under the assumption of small strains, the basic concepts can be applied to this case.

The failure behavior of the material can be separated in three phases (figure 4.3). The diffuse failure phase, weak discontinuity phase and strong discontinuity phase. As it is shown in the next figure, there are clear differences between this stages.

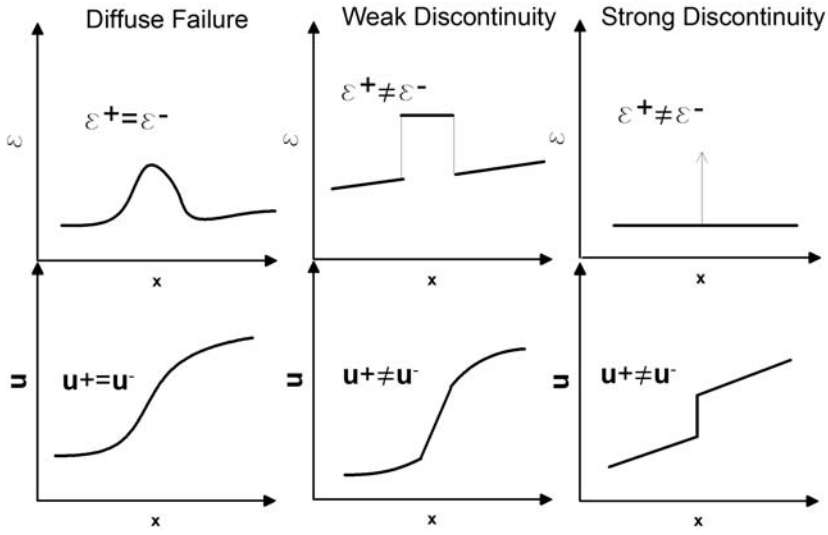

Figure 4.3: Stages in the failure of a material according to fracture mechanics

In the diffuse failure stage, there is a zone where a different behavior from the rest of the analyzed body can be observed. But this zone is not very well defined and it is real difficult to describe how it behaves specifically. Next, is the weak discontinuity stage. In this phase, the failure zone is

now defined between two limits, with a measurable width and a very specific behavior. Finally, is the strong discontinuity phase, in which the failure zone is a fracture near to zero thickness.

In general, in granular materials it is possible to find two out of three of these phases: the diffuse failure and the weak discontinuity stage. The strong discontinuity stage does not occur in this type of material, since it is made out of loose particles that occupies any possible volume, such as a fracture (Figure 4.4).

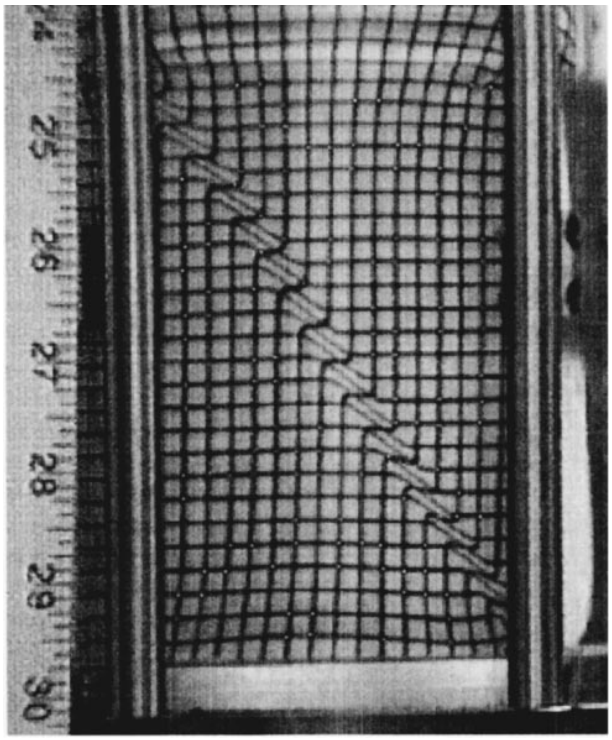

Figure 4.4: Biaxial test in Ottawa Sand with a shear band with a measurable thickness. Alshibli (2003)[8].

There is a body Ω in a time t after bifurcation has occurred, with a shear band π with a normal vector $\mathbf{n}$, and an analysis line called ξ is drawn. The body is separated in two zones (A and B) and the strain rate field is graphed trough the ξ line.

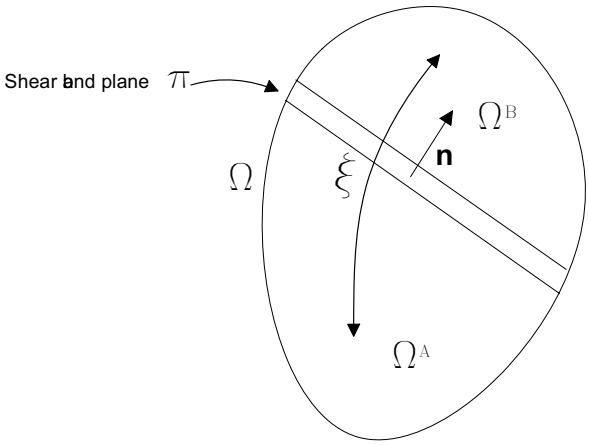

Figure 4.5: Body with a weak discontinuity

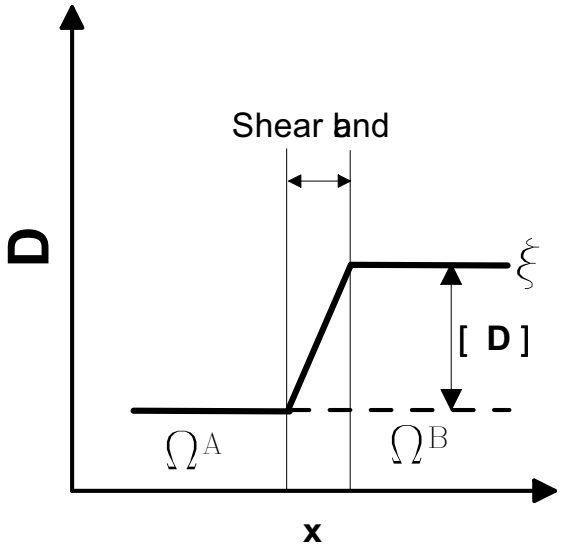

Figure 4.6: Analysis of the stran rate **D** along a ξ line

According to the 4.5 and the 4.6 figures, the strain rate has a constant value at the A zone. In the shear band zone, there is a jump in the strain rate, and in the B zone the value is constant again. This means that if the shear band does not appear, the value of the strain rate will be constant in time t. The strain rate can be supposed as a sum of the homogenous or regular strain rates, and of the shear band or singular strain rate.

$$\mathbf{D}_{\text{total}} = \mathbf{D}_{\text{regular}} + \mathbf{D}_{\text{singular}} \tag{4.3.1}$$

Thus

$$\mathbf{D}_{\text{singular}} = [\![\mathbf{D}]\!] = \frac{1}{2}(\bar{g}\bar{n} + \bar{n}\bar{g}) \tag{4.3.2}$$

If the shear band inclination is assumed constant after bifurcation has occurred, meaning **n** is constant through time, the jump in the strain rate depends only on **g**. Therefore, the jump depends only on the stress state and the strain rate.

To be able to make a numerical implementation on the behavior inside the shear band using the weak discontinuities approach, the UMAT does not only has to calculate if the bifurcation criteria is or is not fulfilled, but it also has to be able to save the direction of the normal vector to shear band and the moment in which the localization occurs.

Once the bifurcation has occurred, the ψ and ϕ angles characterizing the vector **n**, being normal in the shear band, do not allow these values to change anymore. From this moment on, the jump in the strain rate is calculated with equation 4.3.2. Since the coordinate system used to search the bifurcation criterium is rotated, the jump in the strains rate must be rotated to make it coincide with the original coordinate frame as well. With the jump of the strain rate, it is possible to calculate the additional strains and the full strain rate in order to obtain the stresses using the hypoplastic equation.

4.4 Results

4.4.1 Bifurcation

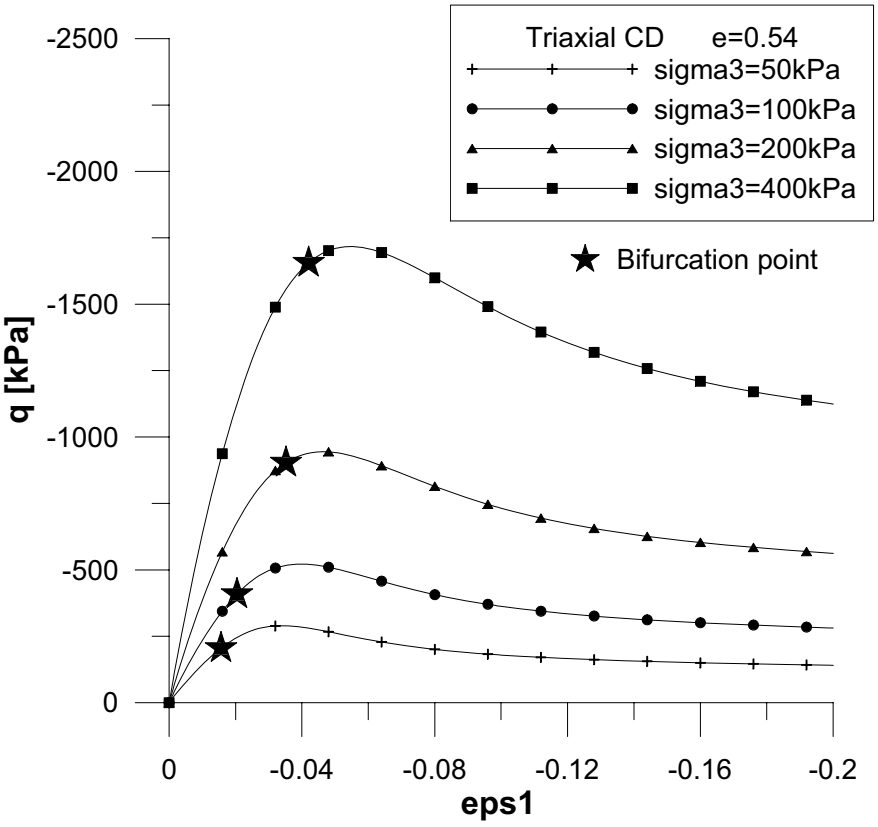

Figure 4.7: CD triaxial test. q vs. ε_1, e=0.54

The results obtained with the simulations (figure 4.7) are in agreement to what the theory says, because the bifurcation point occurs always before the peak state. With the increase of the confinement pressure, the bifurcation occurs at larger strains.

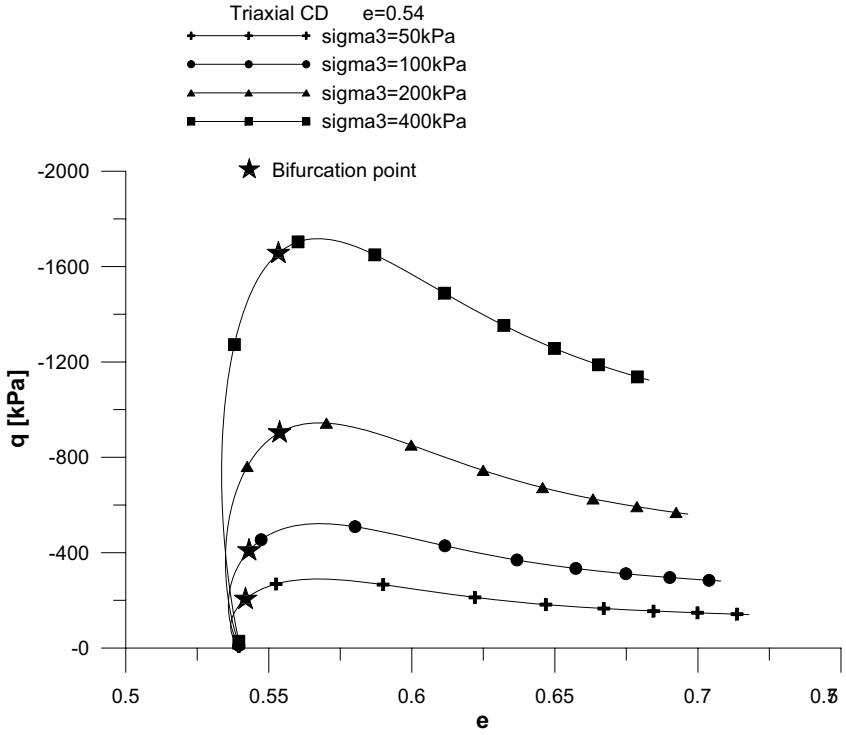

Figure 4.8: CD triaxial test. q vs. e, e=0.54

The bifurcation occurs after the change of phase in the material, meaning that the bifurcation point is located temporally after the material changes from a contractive to a dilatant behavior (figure 4.8).

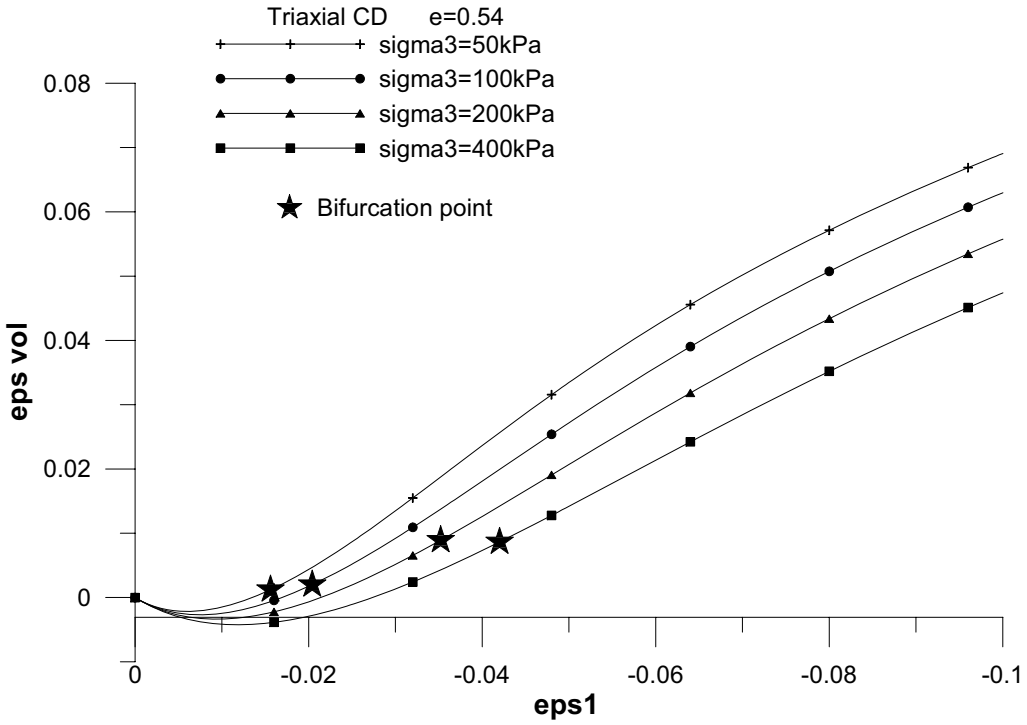

Figure 4.9: CD triaxial test. ε_{vol} vs. ε_1, e=0.54

In the graphic of the response of the material for a confinement pressure of 200 kPa (figure 4.9) shows that if a line is trace through the bifurcation point, the point for this pressure occurs after this line. May be due to an error in the calculations or due to a change in the material after certain pressure.

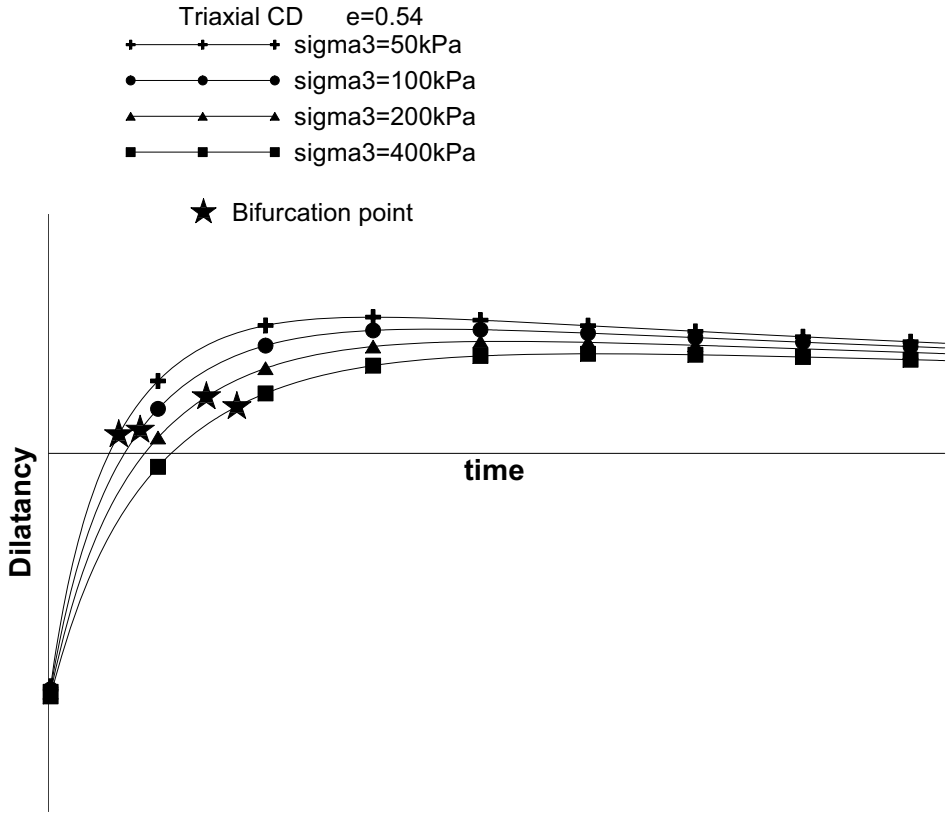

Figure 4.10: CD triaxial test. dilatancy vs. time, e=0.54

In figure 4.10 can be observed the same singularity as the graphic before. The bifurcation point occurs at a higher dilatancy of the material.

4.4.2 Post Bifurcation Behavior

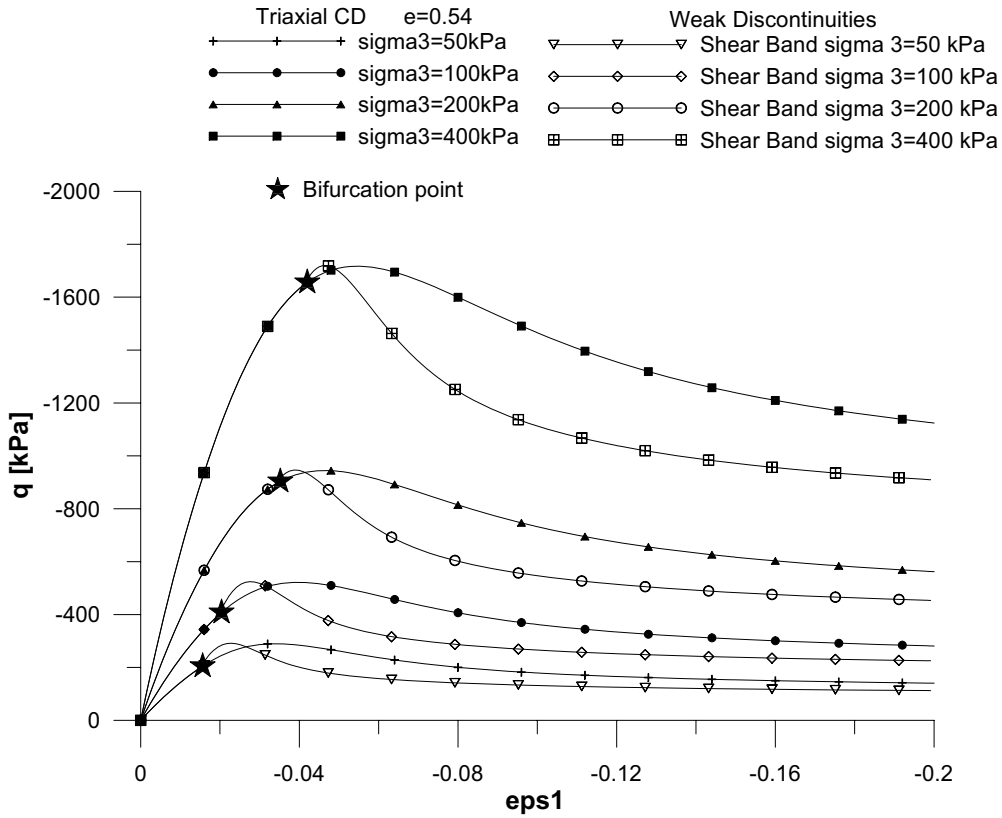

Figure 4.11: CD triaxial test. Post bifurcation. q vs. ε_1, e=0.54

When a post bifurcation behavior is implemented using the weak discontinuities concept, a different response is obtained. The results of the tests are if the whole body analyzed was inside the shear band (figure 4.11). There are several differences between the response of the material in the shear band and the unmodified material. On the first, due to the additional strain rate, the material reaches the peak resistance earlier. This means that the material inside the shear band fails before the other is outside. After the failure, the material inside softens at a higher rate than the one outside. It is also important to remark that with the increase within the confinement pressure, the distance in terms of strain between the peak state inside and outside the shear band decreases. But after the peak state, the behavior changes drastically, because of the softening of the material inside the shear band.

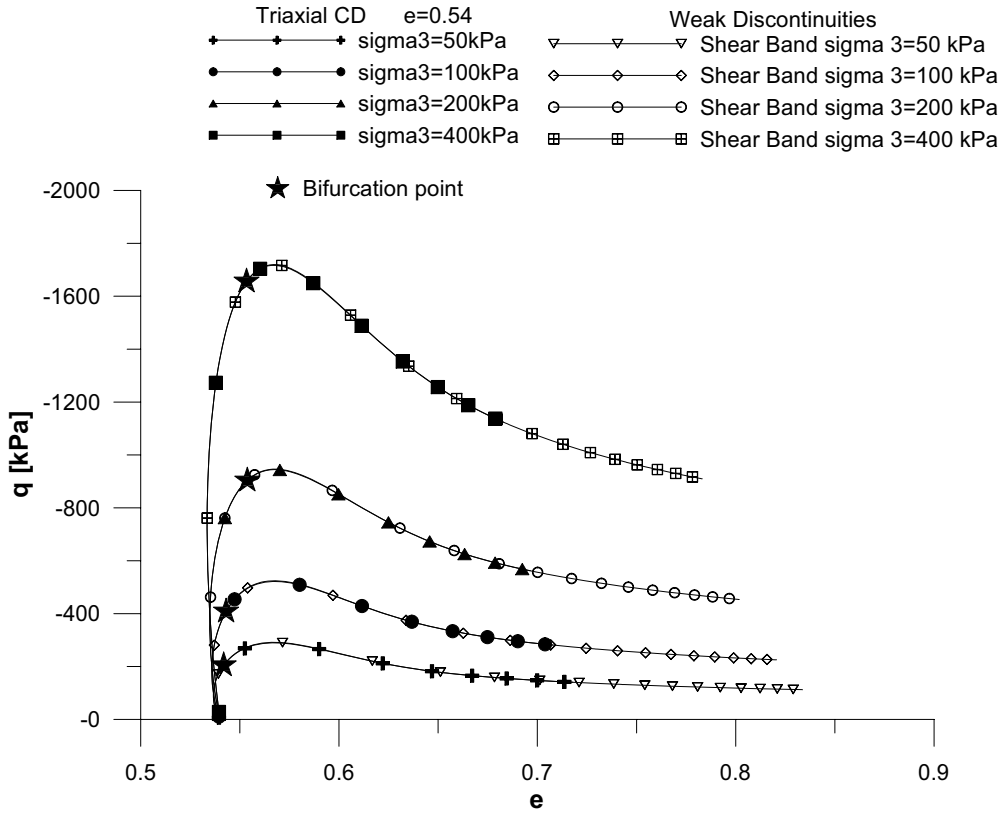

Figure 4.12: CD triaxial test. Post bifurcation q vs. e, e=0.54

It is important to notice that the void ratio inside the shear band is greater than outside (figure 4.12). This is relevant because in the experimental observations made by DESRUES and CHAMBON (2003) (figure 4.13) [3] using computerized tomography they found that the density inside the shear band is lower than the rest of the material. So the results obtained with the simulations agree with the ones obtained experimentally. The difference between the maximum void ratio in the material inside and outside the shear band does not change when the confinement pressure increases. This could mean that the difference is a constant for the material, but experimental measurements must be made to actually determine if this happens.

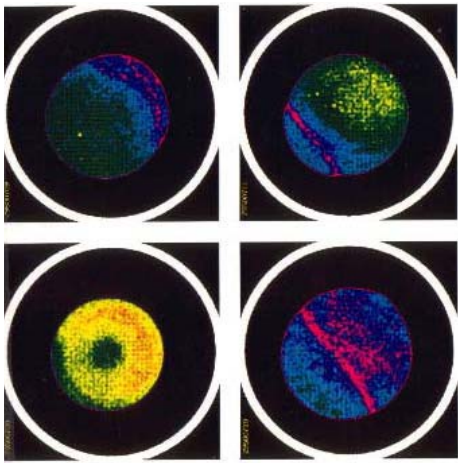

Figure 4.13: Computerized tomography in a triaxial test sample. Shear band can be observed with a lower density.Taken from [3]

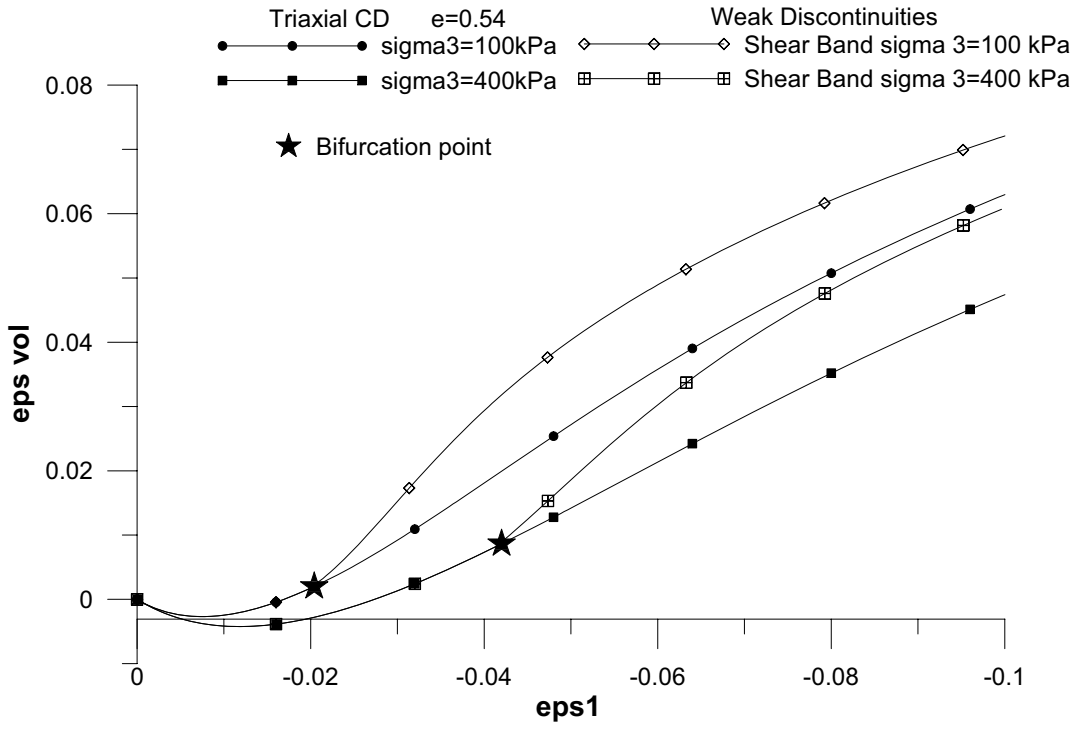

Figure 4.14: CD triaxial test. Post bifurcation ε_{vol} vs. ε_1, e=0.54

In figure 4.14, it can be observed that the volumetric strain in the shear band is greater inside than outside, now that it is positive, consequently the volume, and the void ratio, turn to be greater

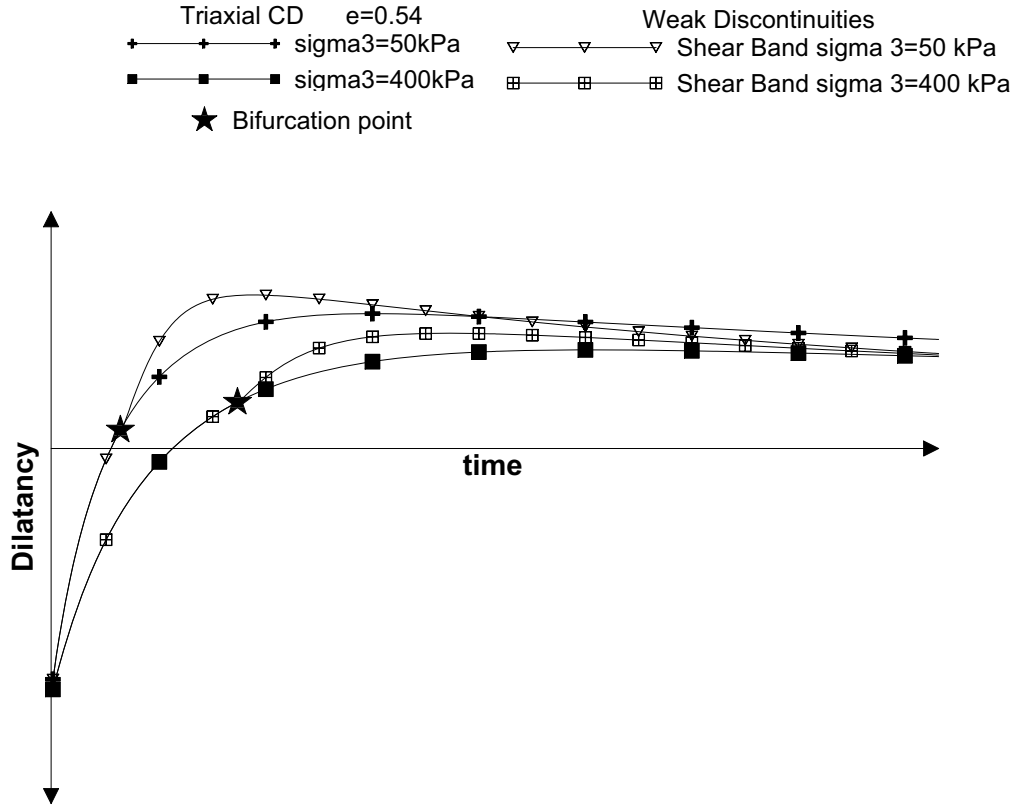

Figure 4.15: CD triaxial test. Post bifurcation. dilatancy vs. time, e=0.54

In figure 4.15, it can be observed that with the increase of the confinement pressure, the volumetric change inside the shear band compared to the material outside is lower. Both the material inside and outside the shear band, and at different confinement pressures, reaches the same stable state, with no changes in regards to dilatancy within time.

Chapter 5

Remarks

The computational implementation made using the methodology proposed by FELLIN [4] produces results that agree with those obtained in experimental results for both undrained and drained triaxial tests. Moreover, due to the simplification done to work with the tensors as vectors, because of the symmetry, the time that takes a simulation to run compared to that one done by FELLIN is approximately half the time.

Since the implementation has been done for the software ABAQUS^{TM}, it can be used for designing or analysis purposes. This could be important since the model can be used in real life problems, furthermore with it, it is possible to obtain reliable results. The finite element application of this model is the final purpose of the computational implementation.

Bifurcation is a theoretical concept aimed to determine the moment in which the localization of the strains starts while the shear band appears at this specific moment. It has not been found if the bifurcation point actually matches the physical appearance of the shear band. With the bifurcation analysis, the direction of the shear band is obtained, which means that the other variable necessary for localization analysis is calculated.

With the weak discontinuities analysis, the complexity of the problem, compared with other methodologies is reduced. Even more, it is easy to implement and the computational cost is very low. Additionally it gives the response of the material inside the shear band. This could be use in finite element analysis, along with a shear band tracking algorithm producing reliable results.

The results obtained with the weak discontinuities extension to the hypoplastic model agrees with those obtained at an experimental stage by other authors, in the sense that the results of the

behavior of the material are the same observed in laboratory tests. Since the instrumentation of a shear band is impossible to perform due to its randomness, the results may only be compared in a qualitative sense. If a finite element analysis with the shear band tracking algorithm is performed, the results may be compared to a real life case, validating its quantitative values.

Bibliography

[1] Pablo Andrés Arias. Modelo de comportamiento de materiales granulares: Estudio y determinación de parámetros, tesis de maestría, 2006.

[2] E. Bauer. Analysis of shear band bifurcation with a hypoplastic model for a pressure and density sensitive granular material. *Mechanics of Materials*, (31):597–609, 1999.

[3] J. Desrues. Tracking strain localization in geomaterials using computerized tomography. *Proc. of the International Workshop on X-ray CT for Geomaterials GeoX 2003*, 2003.

[4] Wolfgang Fellin and Alexander Ostermann. Consistent tangent operators for constitutive rate equations. *International Journal for Numerical and Analytical Methods in Geomechanics*, pages 1213–1233.

[5] Wenxiong Huang. Hypoplastic modeling of shear localization in granular materials. Technical report, Institute of General Mechanics of the Technical University of Graz, 2000.

[6] A. Huespe y M. Dolores G. Pulido J. Oliver. El método de las discontinuidades fuertes en deformaciones finitas. 2002.

[7] A.E. Huespe J. Oliver. Continuum approach to material failure in strong discontinuity settings. *Computer methods in applied mechanics and engineering*, (193):3195–3220, 2004.

[8] Susan Batiste Khalid A. Alshibli and Stein Sture. Strain localization in sand: Plane strain versus triaxial compression. *Journal Of Geotechnical And Geoenvironmental Engineering ASCE*, pages 483–494.

[9] A. Murakami and N. Yoshida. Cosserat continuum and finite element analysis. pages 871–876.

[10] Andrzej Niemunis. *Extended Hypoplastic Models For Soils*. PhD thesis, Institute of Foundation Engineering and Soil Mechanics in Bochum, 2003.

[11] J. Oliver. Topics in failure mechanics.

[12] Jacek Tejchman. Shear localization in granular bodies with micro-polar hypoplasticity, 2008.

[13] W. Wu V. A. Osinov. Strain-gradient extension of hypoplasticity. *Acta Mechanica*, (203):37–47, 2008.

[14] W.Wu and Z.Sikora. Localized bifurcation in hypoplasticity. *International Journal of Engineering Science*, 29(2):195–201.